

# **Dark Matter in Cosmology**

Litsa, Aliki<sup>1</sup>, Bovenschen, Stan<sup>2</sup>, and Heikamp, Marnix<sup>3</sup>

<sup>1</sup>GRAPPA institute, University of Amsterdam, 11572418

<sup>2</sup>GRAPPA institute, University of Amsterdam, 10639578

<sup>3</sup>GRAPPA institute, University of Amsterdam, 11805188

## **Abstract**

## Contents

<b>1 Astrophysical methods in Dark Matter research (Aliko Litsa)</b>	<b>3</b>
1.1 Velocity Dispersion . . . . .	3
1.2 Rotation Curves . . . . .	3
1.3 Gravitational lensing . . . . .	6
<b>2 Cosmological Concepts (Aliko Litsa)</b>	<b>9</b>
2.1 Recombination and the creation of the CMB (Aliko Litsa) . . . . .	9
2.2 Inflation (Aliko Litsa) . . . . .	10
2.3 Baryon Acoustic Oscillations (Aliko Litsa) . . . . .	11
2.4 Hubble measurements (Stan) . . . . .	13
2.5 The $\Lambda$ CDM model (Stan Bovenschen) . . . . .	14
2.5.1 Latest measurements from the Planck telescope (Aliko Litsa) . . . . .	14
2.6 Axionic gauge field inflation (Stan) . . . . .	15
<b>3 Types of Dark Matter (Stan Bovenschen)</b>	<b>15</b>
3.1 Baryonic dark matter (Marnix Heikamp) . . . . .	15
3.2 Hot, Warm or Cold Dark Matter? (Stan Bovenschen) . . . . .	16
3.2.1 Hot Dark Matter . . . . .	16
3.2.2 Cold Dark Matter . . . . .	16
3.2.3 Hot + Cold VS. Warm . . . . .	17
<b>4 Numerical Simulations in Dark Matter Cosmology (Aliko Litsa)</b>	<b>17</b>
4.1 Excluding Hot Dark Matter with Numerical Simulations (Aliko Litsa) . . . . .	20
4.2 Physics beyond the CDM model (Marnix Heikamp) . . . . .	21
4.2.1 Problems on small scales . . . . .	21
4.2.2 Mass of galaxies and dark matter halos . . . . .	23
4.2.3 Considering baryonic matter . . . . .	23
4.2.4 Numerical simulation . . . . .	24
4.3 Effect of baryons on Numerical Simulations (Stan) . . . . .	24
4.3.1 Baryonic matter in hydrodynamics . . . . .	25
4.3.2 Numerical techniques . . . . .	26
4.3.3 Modeling galaxies . . . . .	26
4.3.4 Stellar streams . . . . .	27
4.3.5 Future considerations (Marnix Heikamp) . . . . .	28
<b>5 particle physics solutions</b>	<b>28</b>
<b>6 Modified Newtonian Dynamics (MOND) (Marnix Heikamp)</b>	<b>28</b>
6.1 Milgrom's law . . . . .	28
6.2 Conservation of momentum . . . . .	29
6.3 Gravitational waves . . . . .	29
6.4 Bullet cluster . . . . .	30

# 1 Astrophysical methods in Dark Matter research (Aliki Litsa)

The history of dark matter began in the 1930s, when a Dutch radio astronomer by the name of Jan Oort analyzed numbers and velocities of stars located near the Sun and reached the conclusion that the particular stars appeared to be lacking approximately 30-50% of the matter necessary in order to account for their apparent velocities. In 1933, and shortly after Oort's work, Fritz Zwicky performed similar calculations, and concluded that velocity dispersions in rich galaxy clusters require approximately 100 times more mass in order to ensure that they remain bound. Similar research, including various other astrophysical and cosmological methods, continued more intensely during the following decades, and especially in the 1970s, when researchers attempted to further constrain the existence of such *invisible matter*, using galaxy rotation curves. The following paragraphs contain an overview of the main Astrophysical methods, which established the theory of dark matter in the minds of the scientific community.

## 1.1 Velocity Dispersion

As we mentioned above, the earliest dark matter indications appeared through calculations related to the velocity dispersion of galaxies, and, in particular, those carried out by Zwicky on the Coma Cluster of galaxies [1]. In the particular paper, published in the 1930s, the velocities of galaxies belonging to the cluster were mentioned to differ by at least  $1500 - 2000 \text{ km/s}$ , according to various observations. Assuming that the Coma Cluster had reached a stationary state, Zwicky implemented the Virial Theorem as follows:

$$2E_k = -E_{pot}$$

, where  $E_k$  and  $E_{pot}$  stand for the average kinetic and potential energy per unit mass in the system. The cluster size was approximated with  $R \sim 10^{24} \text{ cm}$ , while including a total number of around 800 nebulae, each with a mass of  $M_n \sim 10^9 M_\odot$ . The additional assumption of uniform mass distribution for the contents of the cluster, yields a total cluster mass of  $M_{CC} \sim 800 \times M_n \sim 1.6 \times 10^{45} \text{ gr}$ . The potential energy of such a cluster is given by:  $V = -\frac{3GM^2}{5R}$ , resulting in an average potential energy per unit mass equal to  $E_{pot} = -\frac{3GM}{5R} \sim -64 \times 10^{12} \text{ cm}^2/\text{s}^2$ . In addition, the average kinetic energy can be expressed as  $E_k = \frac{1}{2}\bar{v}^2 \sim 32 \times 10^{12} \text{ cm}^2/\text{s}^2$ . Using the expression of the virial theorem written above, the final result is:

$$(\bar{v}^2)^{1/2} \sim 80 \text{ km/s}$$

. Such a velocity appears to be very small compared to the Doppler effects of at least 1000 km/s measured from observations of the Coma Cluster. The ultimate conclusion that was drawn from the above was that the average density of the cluster, had to satisfy  $\langle \rho \rangle \sim 400 \rho_{lum}$ . In other words, the real density had to exceed the density of the observed luminous matter by a factor of 400, in order for the cluster to remain bound. If the density failed to comply to this restriction, the 800 nebulae of the cluster would be bound to ultimately disperse and become independent of each other, thus no longer constituting a cluster of galaxies.

At this point it is important to point out the fact that Zwicky's results, as mentioned above, were extremely preliminary, and failed to convince most members of the scientific community at the time. The main reason for that was that the calculation of redshifts for the galaxy-members of the Coma Cluster demanded the use of a Hubble constant that, in the 1930s, was extremely poorly constraint. Furthermore, the uncertainties for the masses of the nebulae comprising the Coma Cluster, weakened the argument for the difference between theoretically predicted and observed velocities even further. Whatever the inaccuracies, Zwicky's attempts constitute one of the first steps towards the exploration of the dark matter theory, and are, therefore, worth mentioning in our review. Similar calculations, making use of more accurate data, have, since, been performed for many more known large structures of matter in the Universe, since Velocity Dispersion constitutes one of the basic indicators for the existence of dark matter.

## 1.2 Rotation Curves

The rotation curve argument is another serious indication for the existence of dark matter in the Universe from the early years of research on the topic [2], until today [3], [4]. Such a curve is essentially a diagram of the rotational velocity versus the distance from the center of a galaxy, as presented in Figure 1, and can be better understood by the following simplified explanation.

In the presence of *only* visible gravitational forces, the virial theorem of hydrostatic equilibrium gives:

$$Mv^2 = \frac{GM^2}{R}$$

or

$$\frac{v^2}{R} = \frac{GM}{R^2}$$

As a result, the *Keplerian rotation curve* follows the relation  $v \propto R^{-1/2}$ . However, the observations do not appear to agree with such a conclusion and, instead of rotation curves which decrease with the distance, they give flat curves, indicating that the velocity has to follow  $v \sim \text{const.}$  instead. From the virial formula above and with a constant velocity, one can also conclude that  $M \propto R$  and, moreover:

$$\frac{dM}{dR} = \frac{v^2}{G}$$

But how can this conclusion be reconciled with the dark matter theory? The essence of the argument supports that the Keplerian curves do, actually, accurately represent reality, but at much larger distances than the ones we are able to observe. Therefore, a logical conclusion indicates the existence of much larger galaxies, where great quantities of dark matter extend far beyond the visible matter, in what can be approximated as a spherically symmetric dark matter halo. The density of such a galaxy can be calculated from:

$$\rho = \frac{1}{4\pi R^2} \frac{dM}{dR} = \frac{v^2}{4\pi G R^2}$$

and, therefore,  $\rho \propto R^{-2}$  beyond the visible radius.

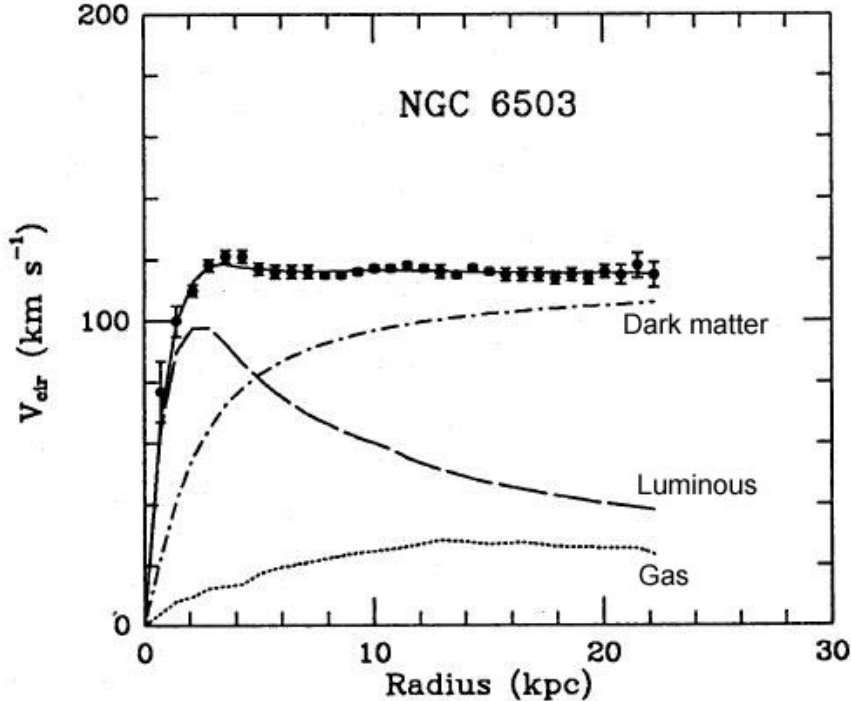


Figure 1: Rotation curve of NGC 6503 [5]

Having, already, given the basis of the Rotation Curve argument in dark matter research, it is important to focus on some more recent results in relation to the same topic. One very important paper to consider is that of McGaugh et al. (2016) [6], which takes one step further in the understanding of galactic rotation. The top panel of Figure 2 presents the rotation curves of three different types of galaxies, while the bottom panel depicts the observed radial acceleration with respect to the radial acceleration of baryonic matter alone. In that same bottom panel, the black line refers to the actual relation of the two types of accelerations calculated, while the dashed line corresponds to the case where all observed acceleration is, essentially, acceleration of baryons. As expected, the baryonic approximation becomes accurate for larger acceleration values, which correspond to smaller radii, and, therefore, to distances from the center of the galaxy where baryons overpower dark matter. On the other hand, in the regime of small accelerations, which probe distances that are closer to the halo, baryons can no longer play a significant role, and the two lines drift apart. From the particular figure it

is, also, straightforward to conclude that, as galaxies get more and more faint (with the gas-dominated dwarf being the faintest), the observed acceleration reaches smaller and smaller values, which indicates that dark matter overpowers the galactic compositions. A result like that is completely justified, since a galaxy which is fainter is, also, bound to include less luminous/baryonic matter.

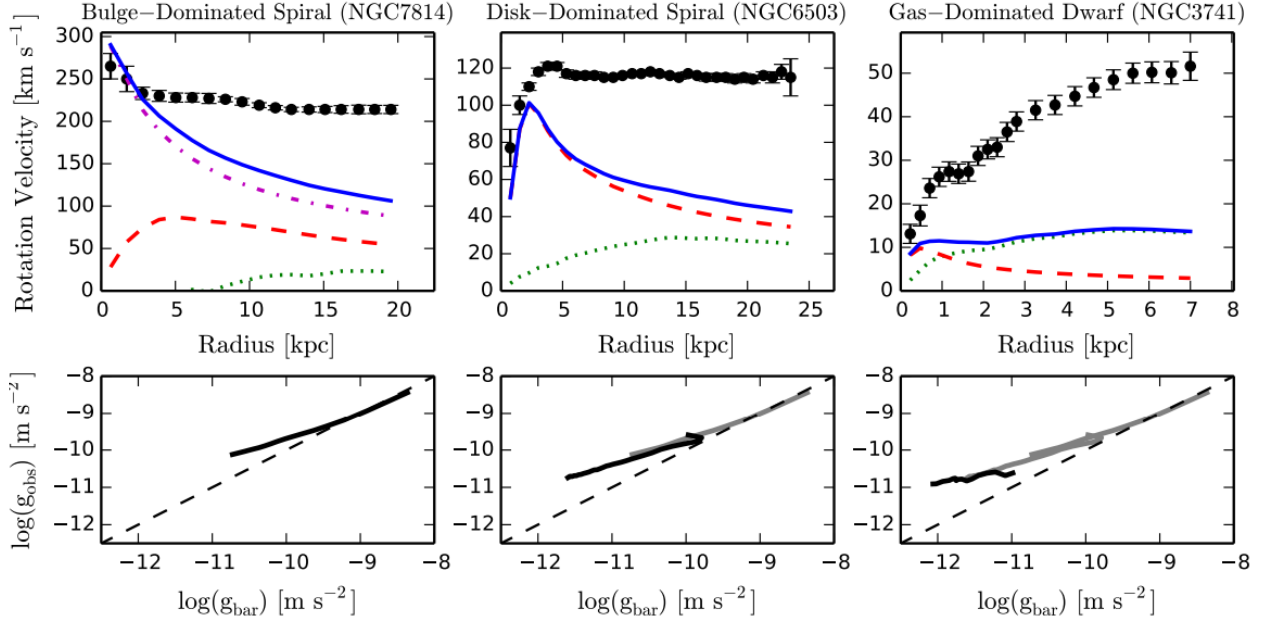


Figure 2: Top panel: Rotation Curves of individual galaxies. Each baryonic component is represented: dotted lines for the gas, dashed lines for the stellar disk, and dash-dotted lines for the bulge, when present. The sum of these components is the baryonic mass model (solid line). Bottom panel: Relation of observed radial acceleration to baryon radial acceleration. The solid line is the actual relation, while the dashed line corresponds to unity. From left to right each line is replotted in gray to illustrate how progressively fainter galaxies probe progressively lower regimes of acceleration. [6]

Another significant result of the particular paper is presented in Figure 3, where the relation of the observed radial acceleration (from rotation curves) and the baryonic acceleration (from the solution of the Poisson equation) is plotted for 153 different galaxies. The resulting diagram indicates an extremely significant correlation between the two values, whose physical causes have yet to be explained with absolute certainty. A very intriguing fact which is worth mentioning is that the line created by the data points is predicted by Modified Newtonian Dynamics theories - the counter-argument to dark matter - which will be explained more thoroughly in section 6. Another possible explanation lies in small-scale structure formation, and indicates that it is the specific initial conditions of this procedure that have been imprinted on all galaxies which have arisen from it, thus interconnecting their properties. Whatever the true cause of the correlation, such a result indicates an unknown side of physics, which has yet to be discovered.

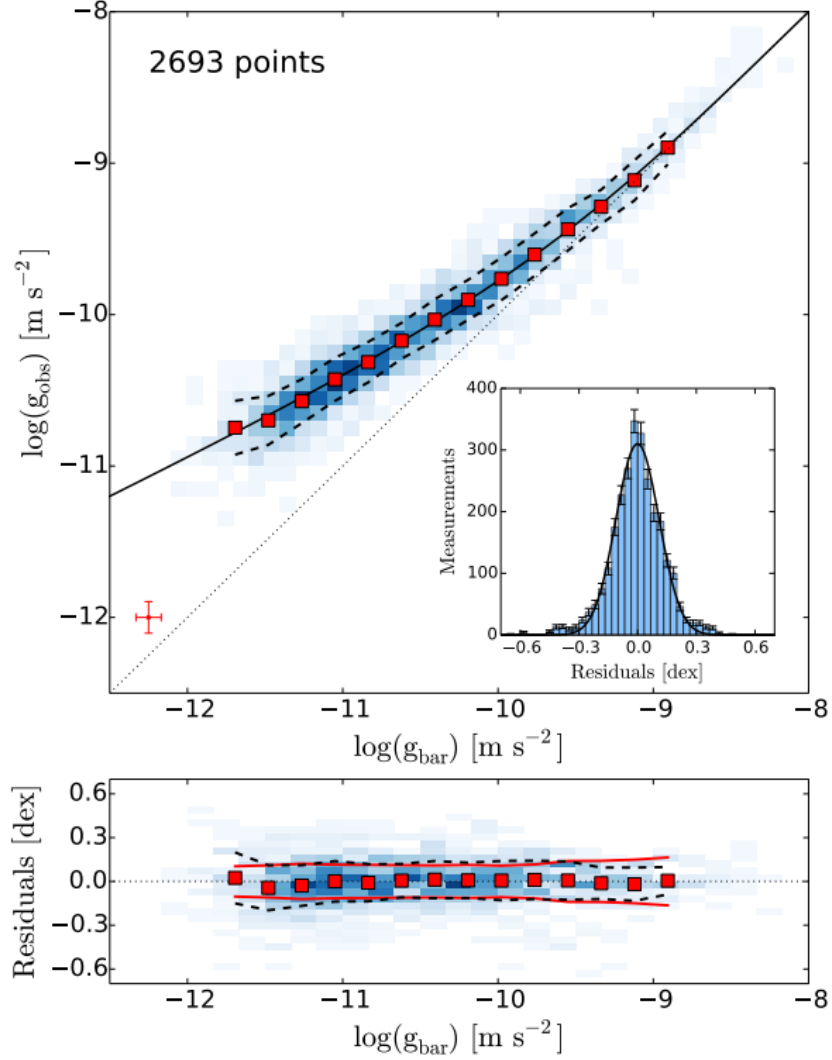


Figure 3: The centripetal acceleration observed in rotation curves,  $g_{\text{obs}} = V^2/R$ , is plotted against that predicted for the observed distribution of baryons,  $g_{\text{bar}}$  in the upper panel. Nearly 2700 individual data points for 153 SPARC galaxies are shown in grayscale [6]

### 1.3 Gravitational lensing

Another astrophysical method that has been extremely important for the establishment of the dark matter argument is that of gravitational lensing, and especially of the weak gravitational lensing. More specifically, Gravitational lensing is one of the various predictions made in Albert Einstein's theory of General relativity and refers to the deflection of light by gravitational fields, as well as to the resulting effect of that deflection on images seen by an observer. In Figure 6 we can see a simple depiction of the gravitational lensing effect, in the case of light rays travelling from a distant quasar and being deflected by a galaxy-lens. The result is the creation of two *false images* of the quasar, which are observed from Earth, and give a false perception for the position of the quasar object on the celestial sphere. In Figure 4, we, also, present an example of strong gravitational lensing from Abell S295, where the two "false" images can, also, be observed very clearly.

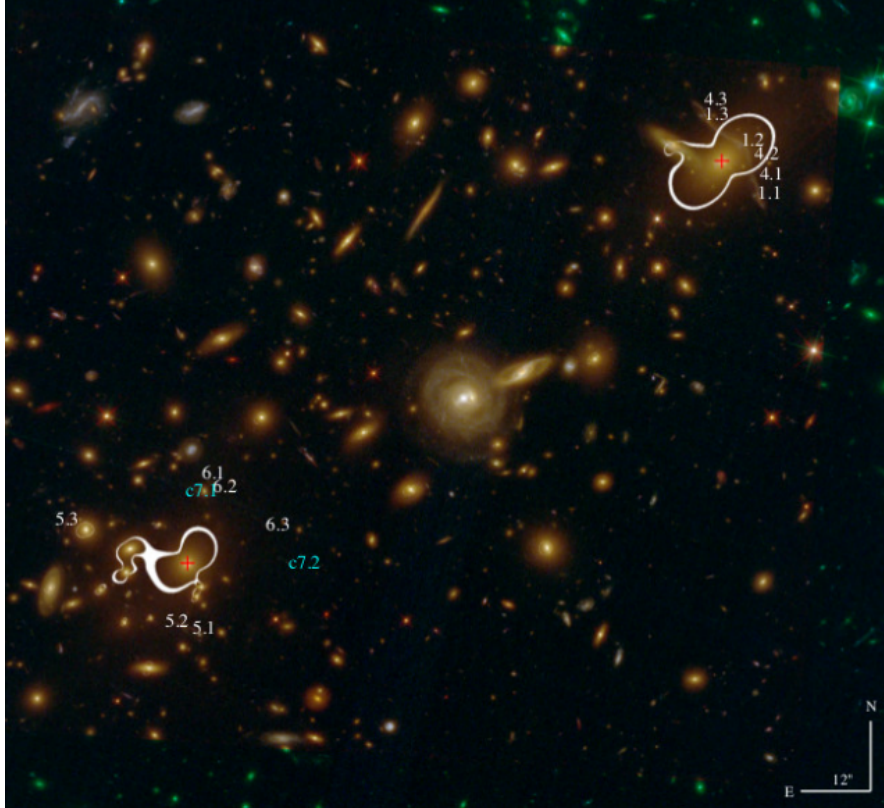


Figure 4: Strong gravitational lensing in Abell S295 [7]

There exist various different types of gravitational lensing, depending of the strength of the effect and on the corresponding degree of image distortion of distant objects, including strong gravitational lensing, weak gravitational lensing and gravitational micro-lensing. More specifically:

- **Strong gravitational lensing**, in which case the mass of the lens is enough to produce multiple images, arcs, or even Einstein rings. Generally, the strong lensing effect requires the projected lens mass density greater than the critical density  $\Sigma_{cr}$ . For point-like background sources, there will be multiple images; for extended background emissions, there can be arcs or rings.
- **Weak gravitational lensing**, in which case the mass acting as a lens causes disfigurements to the background objects that are observed, but is not strong enough to produce arcs or rings.
- **Gravitational microlensing**, in which case the lens allows the observation of sources producing little or no light, due to the collection and beaming of emitted light towards the direction of the observer.

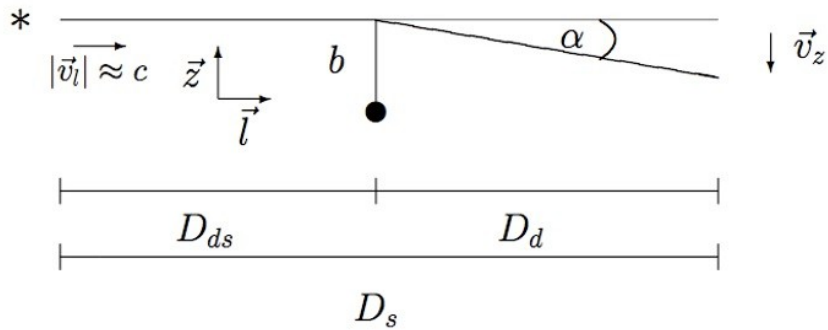


Figure 5: Deflection of a light beam originating from a point-like source

In order to better understand the concept of gravitational lensing, we will attempt to present the simple basis of the argument using Einstein's theory of General Relativity, using light originating from a point-like

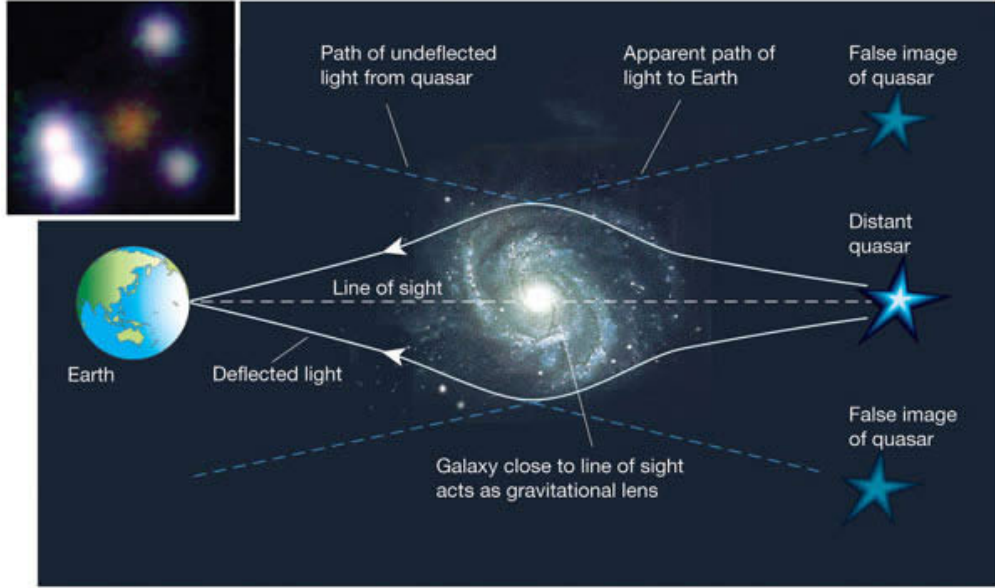


Figure 6: Lensing effect (*taken from <https://pics-about-space.com/gravitational-lensing-and-dark-matter>*)

source. The deflection angle  $\alpha$  can be calculated from:

$$\vec{\alpha} = \frac{4GM}{c^2 b}$$

where  $b$  is the distance from the point-like source of the beam to the observer.

If we consider the gravitational field as an optical medium with an index of refraction  $n > 1$ , the particular index is such that the light beam travels slower through the medium than through vacuum, and is given by (Ehlers & Schneider 1992 [8]):

$$n = 1 - \frac{2}{c^2} \Phi = 1 + \frac{2}{c^2} |\Phi|$$

where  $\Phi$  refers to the gravitational potential. Furthermore:

$$\vec{\alpha} = - \int \nabla_{\perp} n dl = \frac{2}{c^2} \int \nabla_{\perp} \Phi dl$$

which contains the integral of the potential gradient perpendicular to the light propagation direction ( $\nabla_{\perp} \Phi = \frac{d\Phi}{dz}$ ). Therefore, for a light beam traveling at a distance  $b = R_{\text{sun}}$  from the center of the sun (which is considered as a point-like source), the deflection angle  $\alpha$  is calculated to be approximately  $1.7''$ . Further topics that are related to Gravitational lensing include the lens equation, as well as the phenomenon that is known as the *Einstein ring*. However, such discussion goes beyond the purposes of the particular review.

The method of gravitational lensing can, also, be applied in *Bullet Cluster* observations, where two clusters are undergoing high-velocity collisions, and, subsequently, emit X-rays that have been detected by the Chandra telescope. The interested reader can find out more by reading [9, 10, 11]. In images of such phenomena that have been captured, we can observe two different types of material. The *hot gas* is concentrated at the collision front, while some dark matter, confirmed by weak gravitational lensing techniques, is concentrated behind the collision front (Figure 7). We can, therefore, conclude that the dark matter detected in such phenomena, not only exists, but is also collisionless.

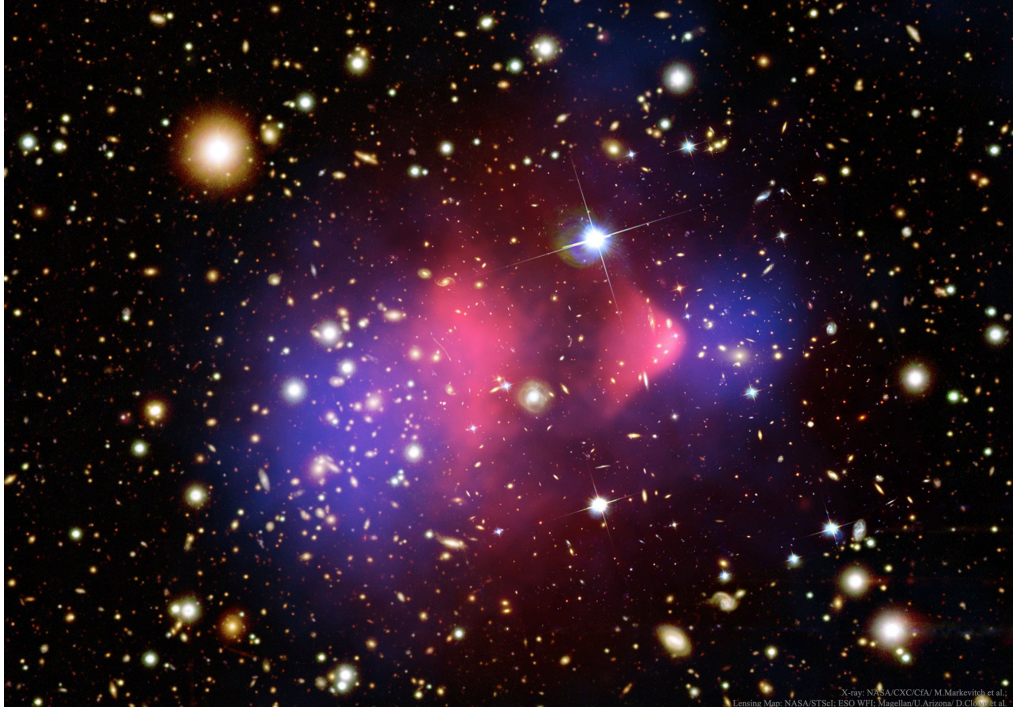


Figure 7: Bullet Cluster 1E0657-558. Blue refers to the collisionless dark matter and red to the hot baryonic matter in the collision front. Image provided courtesy of Chandra X-ray Observatory. [12]

## 2 Cosmological Concepts (Aliki Litsa)

The deeper understanding of dark matter physics, also, requires a good understanding of the cosmological concepts of inflation, as well as those of Baryon Acoustic Oscillations and the Cosmic Microwave Background. The following paragraphs contain a brief overview of the main knowledge necessary for dealing with the topics of this review.

### 2.1 Recombination and the creation of the CMB (Aliki Litsa)

The history of the Universe begins at time  $t = 0$  with the Big Bang, and continues until today at  $t \sim 10^{10} \text{ yr}$ . During the early stages of cosmological evolution, the Universe was hot and dense, and consisted of a hot, ionized plasma, where baryonic matter and radiation were strongly coupled together. While the temperature of the Universe exceeded the value of  $\sim 4 \times 10^3 \text{ K}$ , the formation of neutral atoms from electrons and protons remained impossible, due to the extremely high energies of the plasma, which surpassed the hydrogen binding energy. Under such circumstances, the electron number density remained very high and, due to the continuous electron-photon interactions via Thomson scattering, limited the mean free path of photons considerably, thus keeping them from travelling independently of the matter component.

When the age of the Universe reached  $377000 \text{ years}$  the temperature, finally, dropped below  $4 \times 10^3 \text{ K}$  and, as a result, electrons joined protons in order to create neutral atoms. The particular phenomenon is called recombination, and resulted in the significant drop of the electron number density, allowing photons to escape the plasma and travel freely in the Universe. The same radiation, which was released during this *photon decoupling*, is still measured today at a temperature of  $\sim 2.7 \text{ K}$  and is known as the Cosmic Microwave Background (CMB). A picture of the CMB as measured by the Planck telescope is shown in Figure 8.

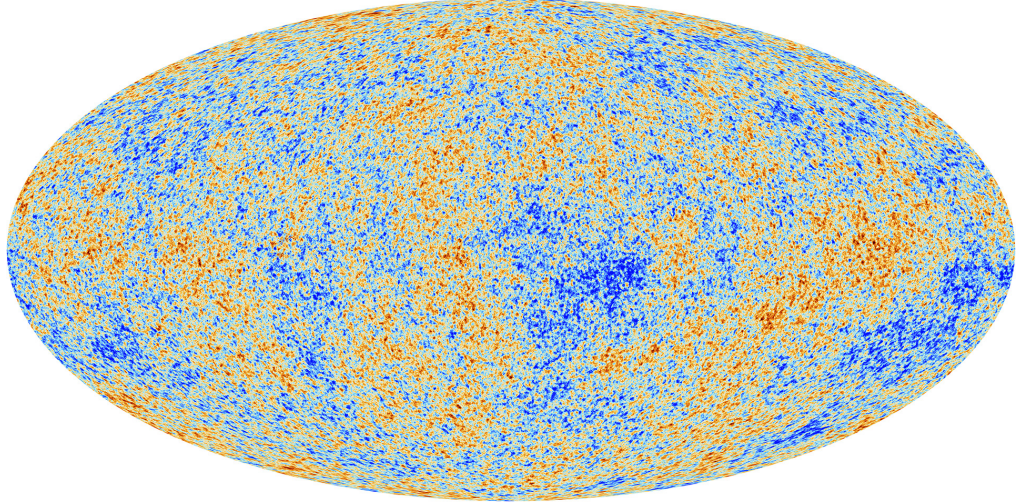


Figure 8: The anisotropies of the CMB radiation as measured by Planck. Taken by: <https://www.esa.int>

## 2.2 Inflation (Aliki Litsa)

Another extremely important concept, which is necessary for the understanding of the transformation of the Universe into the form which we observe today, is that of the inflation mechanism. But why is such a mechanism's existence required in our Cosmological Model?

According to measurements of the CMB radiation made by the Planck telescope and its predecessors, the Universe appears to be homogeneous and isotropic on large scales, up to a factor of  $10^{-5}$ . Such a uniformity can, only, be achieved if the furthest regions of the Universe have already been in causal contact in the past. More specifically, such a uniformity indicates that light must have been able to travel across all these uniform regions in the past, thus smoothing out any prominent inhomogeneities. Such a causal contact cannot be explained by the basic cosmological theory and gives rise to what is known as the horizon problem. Figure 9 presents the horizon as seen by an observer today (at point A) looking towards the time of decoupling. Observers B and C exist at the time of decoupling and have independent horizons that do not intersect with each other, thus containing regions which are not in causal contact. Despite the fact that the regions seen by observers B and C at the time of the CMB release appear to be entirely detached from each other, observer A witnesses a CMB which is extremely uniform.

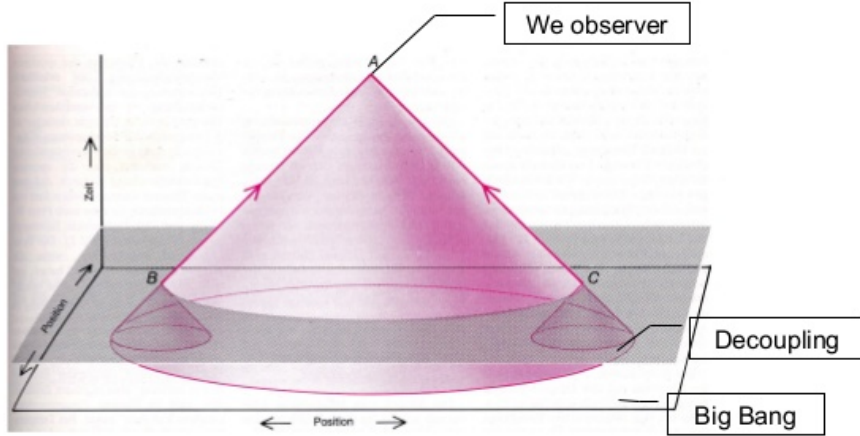


Figure 9: The horizon problem

The solution to the problem is given by the inflation mechanism, which provides an exponential expansion of the Universe at negative conformal time, even before the Big Bang event. According to the inflation

scenario, all regions were in causal contact, inside the Hubble sphere at some point in the past. However, due to such an accelerated expansion many regions exited the Hubble sphere (the *causal contact sphere*), and thus appeared as though causally disconnected at the time of the Big Bang and of recombination.

However, the "blessings" of the inflation mechanism are not strictly limited to the solution of the horizon problem. The Planck telescope and its predecessors have measured a Universe which is very close to perfectly flat. Such a result can easily be explained with an accelerated expansion theory, which stretches the various modes, and "deprives" them of all curvature. Furthermore, inflation is able to produce the very precise initial conditions necessary, in order for structure formation to take place and result in the creation of the Universe as it is observed today (more on structure formation in section 4). It, therefore, solves the *fine-tuning* problem, and provides the seed for large-scale structure formation in the form of adiabatic density perturbations.

### 2.3 Baryon Acoustic Oscillations (Aliki Litsa)

Having already mentioned various astrophysical methods of establishing the credibility of the dark matter argument in section 1, it is time to move on to some cosmological phenomena. The Baryon Acoustic Oscillations are those that give rise to the various acoustic peaks in the Cosmic Microwave Background power-spectrum [13]. Their creation took place in the Early Universe, before the recombination of electrons and protons for the formation of neutral hydrogen atoms and the subsequent release of the CMB radiation. During this early age of the Universe, the various cosmological perturbations caused the excitation of sound waves in the relativistic plasma. The particular sound waves resulted in the oscillation of modes, which arose from the constant "struggle" between the gravitational potential and the radiation pressure. Figure 10 depicts the particular "struggle", where the radiation pressure pushes the oscillating modes out of the gravitational well, and the gravitational potential acts as a restoring force by dragging them back in. Until the time of recombination all the various modes of different wavelength had completed a different number of oscillation periods, a fact that has been "captured" in the CMB power spectrum as the different maxima and minima shown in Figure 11. While, however, the baryon perturbations travelled outwards in the form of an acoustic wave, the dark matter perturbations grew in place. At the time of recombination, the speed of sound falls rapidly, which results in the end of the sound-wave propagation, at a moment when the baryon acoustic shell has expanded to a radius of  $\sim 150 \text{ Mpc}$ . It is after the time of recombination at redshift  $z \sim 1100$  that dark matter perturbations, along with the baryonic perturbations contribute to the creation of all large-scale structures observed in the Universe today. If dark matter failed to exist, and its corresponding perturbations failed to dominate over the baryonic acoustic perturbations, the resulting structures created would have to be much larger than the ones observed today. We can, therefore, confirm the existence of an additional component, apart from regular (baryonic) matter itself, that is essential in accounting for the cosmological structure witnessed. Such a conclusion provides a strong ally of the dark matter argument, from a cosmological perspective.

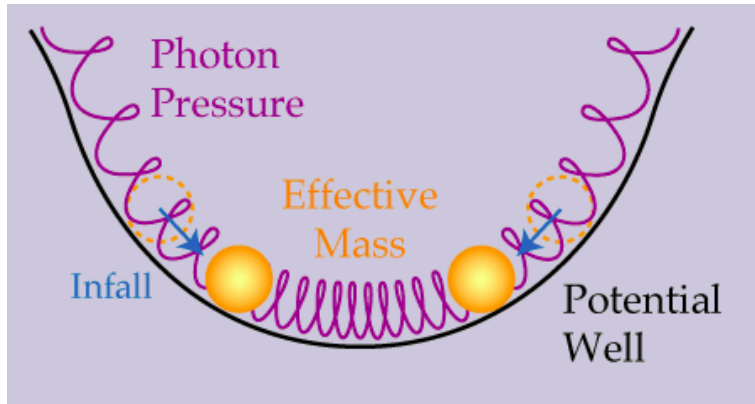


Figure 10: Baryon Acoustic Oscillations: the gravitational potential drags modes inside the well, while the radiation pressure pushes them out. Taken from: <http://background.uchicago.edu/whu/physics/acoustic.html>

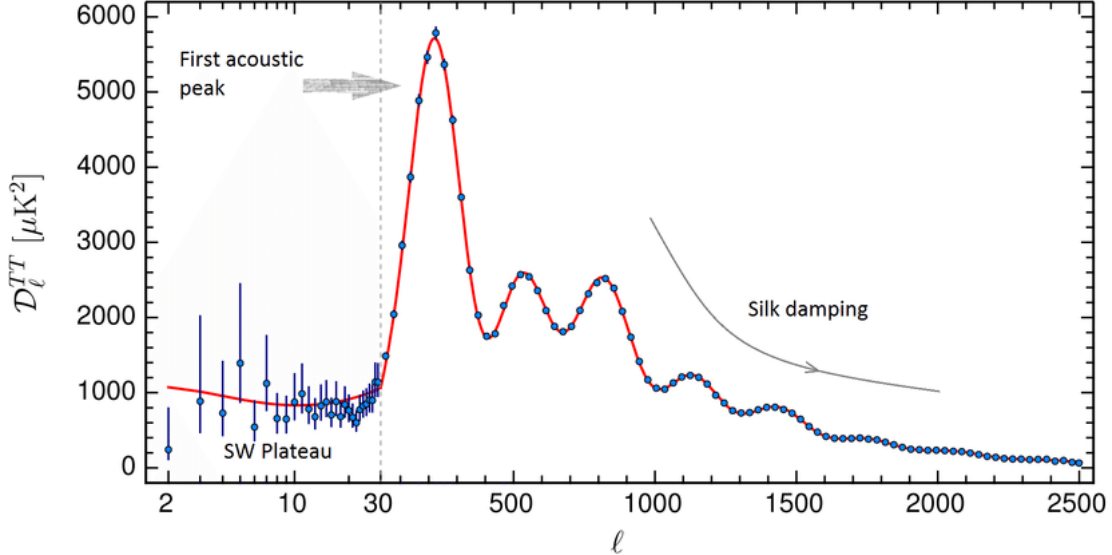


Figure 11: The CMB anisotropy power spectrum found by the Planck collaboration [14]

Of all the peaks in the CMB anisotropy power spectrum, it is the third peak that can provide us with information related to the dark matter component in the Universe. More specifically, having a third peak with an amplitude that exceeds that of the second peak, is a clear indication of the contribution of dark matter density to the system, due to reasons that will be explained in the following. The third peak of the CMB power spectrum corresponds to modes that have completed more oscillations compared to the first two peaks, or, in other words, have began oscillating earlier on, during the radiation domination era. During the particular era radiation pressure dominates compared to the gravitational potential, and the potential decays, driving the oscillation amplitude of baryons up. Since this *driving effect* cannot have a large influence when the Universe becomes matter dominated and the gravitational potential is significant, the second peak does not experience a similar rise in amplitude. As a result, the third peak, which corresponds to radiation domination, is expected to overpower the second one, which captures oscillations in the matter - and, therefore, dark matter - domination period.

At this point it is, also, important to point out another very interesting fact about Baryon Acoustic Oscillations. We have, already, mentioned how these oscillations are imprinted on the CMB anisotropy power spectrum shown above, as all the different maxima and minima observed. Another very significant effect of these oscillations is that they are, also, imprinted on the late-time power spectrum  $P(k)$  of the non-relativistic matter in the Universe [15], [16], [17], [18], at the exact positions corresponding to the oscillation peaks in the CMB anisotropy power spectrum. The matter power spectrum, as shown in Figure 12, corresponds to the matter perturbation squared and is calculated by:  $P_\Delta(k, z) = |\Delta_{m,k}(z)|^2$ . We can, therefore, observe how the baryon acoustic oscillations, not only have affected the temperature fluctuations found in the Cosmic Microwave Background, but also the layout of the matter component in the Universe itself. A notion like that appears to be reasonable, since an oscillation of baryonic matter is bound to have an influence on the distribution of the particular matter.

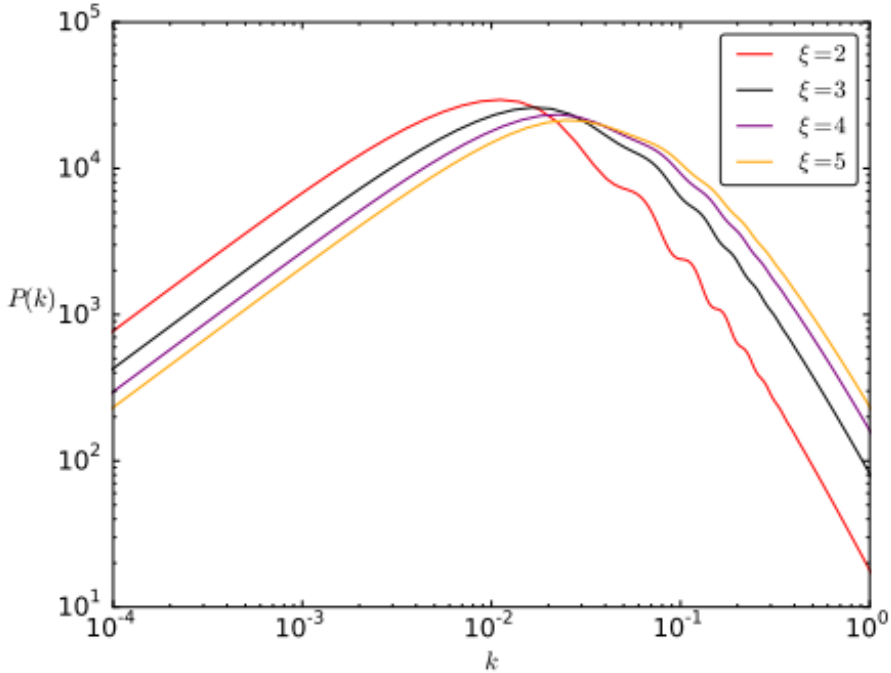


Figure 12: The matter power spectrum [19], where  $\xi = 3$  corresponds to the Universe as we know it. Visible are small amplitude baryon acoustic oscillations in the spectrum.

## 2.4 Hubble measurements (Stan)

It is well known that the Hubble parameter measures how fast the universe is expanding at a given age of the universe. With the Hubble parameter today, the Hubble constant, we are able to make an estimate of the age of the universe by calculating how long it took the universe to expand to this point. The most common way of measuring the Hubble constant is by using supernovae Ia as standard candles. The magnitudes of supernovae type Ia well known and therefore we can calculate the distance to it. Also we know the redshift of the supernovae and thus we can calculate the Hubble constant. This method is a direct measurement in the local universe. The most precise measurement today is [20]:

$$H_0^{local} = 73.24 \pm 1.74 \text{ km} \cdot \text{s}^{-1} \text{Mpc}^{-1}$$

Another way of measuring is the indirect way of measuring the Hubble constant. This method uses observations of the CMB and large scale structures. The observations of the CMB powerspectrum from the Planck telescope are well in line with the spatially flat  $\Lambda$ CDM model. The Hubble constant calculated from these observations however are not consistent with the above mentioned local observations [21]:

$$H_0^{Planck} = 67.8 \pm 0.9 \text{ km} \cdot \text{s}^{-1} \text{Mpc}^{-1}$$

Ofcourse it is wrong that those values are not the same. The first thing to check are the systematic errors in either the CMB measurements or in the local measurements. As the values got more precise the discrepancy did not disappear. The newly calculated Hubble constant is still  $3.1\sigma$  larger than the Hubble constant from the updated Planck measurements [22]. Since the Planck values of the Hubble constant arise by assuming the  $\Lambda$ CDM model, an other possible explanation could be that the  $\Lambda$ CDM model is just not right.

A possible solution could be that the local universe is different than the global universe. If the local universe has an underdensity this could cause the local Hubble constant to be higher. A region with lower density expands faster therefore it looks like the age of the universe is less since it takes less time to expand to a certain volume. We know that the Hubble constant goes as  $H_0 \propto \frac{1}{\tau_{universe}}$ , therefore  $H_0$  will be higher in the local universe. This has been investigated by using local inhomogeneities on the luminosity distance. It turns out that the radial profile has an underdensity of 300 Mpc/h in one direction [23]. This fluctuation

in luminosity distance is related to the Hubble parameter by:

$$\frac{\Delta H(z)}{\bar{H}_0} = -\frac{\Delta D_L(z)}{\bar{D}_L(z)} = -\frac{1}{3}f\bar{\delta}$$

where  $\bar{\delta}$  is the average density contrast over a co-moving sphere. In figure 13 this relation is shown. We clearly see an underdensity at  $0.1 < z < 0.4$ . This results in a higher Hubble parameter in this region. At higher  $z$  we see no fluctuation anymore since the local underdensity is negligible on global scale.

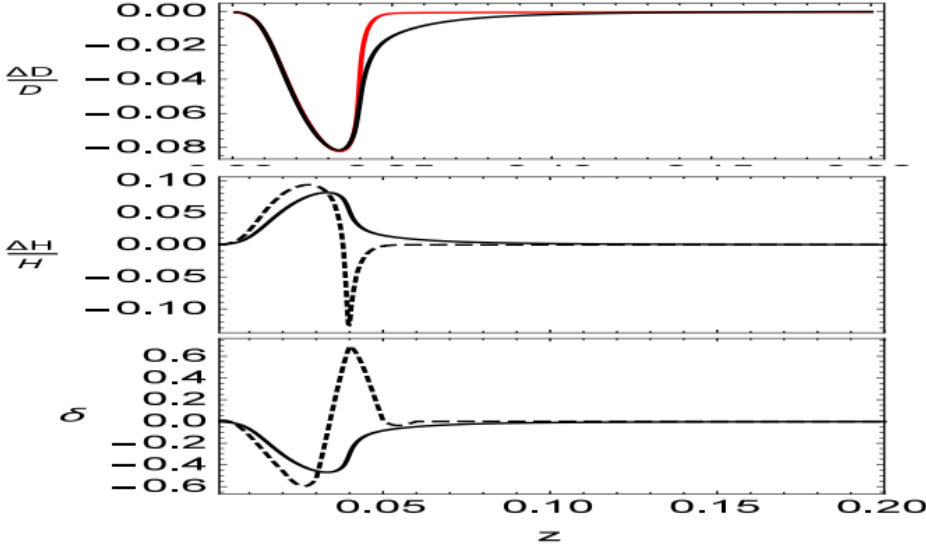


Figure 13: Relation between inhomogeneities in luminosity distance and inhomogeneities in values of the Hubble constant due to a local underdensity. The dashed line is the Newtonian limit of the cosmological scalar perturbation theory [23].

Whether or not this application of the  $\Lambda$ CDM model can explain the total discrepancy of the Hubble constant remains the question. Other approaches, based on perturbation theory or by using N-body simulations, have also been investigated extensively. See [24] for a comparison between those two approaches.

## 2.5 The $\Lambda$ CDM model (Stan Bovenschen)

$\Lambda$ CDM is a model which combines the components of dark energy and cold dark matter, and the most plausible model of the Universe today. Cold dark matter is explained in section 3.2.2. In order to know what amount of dark matter and dark energy we are looking for we can measure the density parameter  $\Omega$ :

$$\Omega = \frac{\rho}{\rho_c} = \frac{8\pi G\rho}{3H_0^2}$$

The fact that we are measuring a component of the density parameter  $\Omega_\Lambda > 0$  means that there is some dark energy in the universe. Hence we have to use the  $\Lambda$ CDM model.

### 2.5.1 Latest measurements from the Planck telescope (Aliki Litsa)

The measurements made by the Planck telescope [14] are constraint using all astrophysical methods mentioned in section 1, as well as the Baryon Acoustic Oscillation information mentioned above. Some additional constraints are calculated using distance and velocity measurements of Type Ia Supernovae - the "standard candles" of astrophysical observations - as explained in section 2.4. The total energy density of all components, considering a flat universe, is expected to be  $\Omega_{tot} \sim 1$ . According to measurements of the telescope made in 2015, the rest of the components have the following characteristic values:

- The energy density of baryonic matter:  $\Omega_b h^2 \simeq 0.02230 \pm 0.00014$
- The energy density of cold dark matter:  $\Omega_c h^2 \simeq 0.1188 \pm 0.0010$

- The energy density of dark energy:  $\Omega_\Lambda \simeq 0.6911 \pm 0.0062$
- Hubble's constant at the present time:  $H_0 \simeq 67.74 \pm 0.46 \text{ km/s/Mpc}$
- The energy density of all matter in the universe  $\Omega_m = \Omega_c + \Omega_b$ :  $\Omega_m \simeq 0.3089 \pm 0.0062$

The values above constitute most of the essential characteristics of the  $\Lambda CDM$  model, and express the contribution of each of the components to the content of the Universe. Some of the problems of the particular model will be discussed in the following sections of the review.

## 2.6 Axionic gauge field inflation (Stan)

Caldwell 2018

# 3 Types of Dark Matter (Stan Bovenschen)

In the previous chapter we have seen several explanations why we think dark matter exists. Now we want to prove this by finding actual dark matter. To be able to start looking for dark matter we first have to know where to look for.

In this chapter we will narrow down the possible consistencies of dark matter by explaining whether or not dark matter consists of baryons. We will also discuss some dark matter models from which we can extract the consistence of dark matter. Finally we will show the current status of the field by displaying some measurements.

## 3.1 Baryonic dark matter (Marnix Heikamp)

We have already seen that there must exist dark matter, but we have yet to determine what kind of matter dark matter consists of. There are various possibilities of matter to consider, some of which will be discussed below, along with the likelihood of dark matter to be composed by them.

The simplest thing to assume is that dark matter consists of ordinary baryons, that we haven't found yet. We have already seen an argument against baryonic dark matter in section 2.3, but we will provide two more:

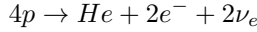
- **The amount of baryons.** There exist two ways in which we can measure the amount of baryons that are present in the universe. Firstly, we can measure the abundance of light elements, specifically deuterium. This abundance is closely governed by the amount of baryons that exist. Secondly, we can consider the distribution of hot and cold spots in the CMB. Both of these turn out to be in excellent accordance with one another. As we saw, the energy density for baryonic matter is  $\Omega_b = 0.02230/0.49 \approx 0.05$ , whereas the total energy density of all matter in the universe is approximately 0.30.
- **Various candidates are unlikely**
  - **Hydrogen or helium gas** When hydrogen is frozen, it forms 'snowballs' which would evaporate and thus do not contribute. When helium is in a cool state, it should absorb light that comes from behind it, but this is scarcely witnessed. When there's hot gas, this should emit X-ray radiation, but this is also scarce.
  - **Dusts, rocks or asteroids** More complex elements may create bigger objects, such as rocks or asteroids. However, that would imply that stars should also have higher metalicity than is the case. This is thus not likely. For dust to be present, we should have more blocking of light, which is not abundant. So, also baryonic dust cannot be the constituent of dark matter.
  - **MACHOs.** MACHOs, very low luminosity stars are hard to witness, for apparent reasons. They can be found using gravitational microlensing. Although some have been found over the last decades, it does not nearly come close to explaining all the missing matter in the Universe.
  - **Very massive objects.** The remnants of very massive stars that formed early in Galactic history might form neutron stars and massive black holes. For neutron stars to form, a star usually goes supernova, ejecting many heavy elements into the Universe, which we don't observe. Additionally, the final mass of a neutron star is not high enough to explain all the missing matter. Very massive stars usually end their lives by collapsing into a black hole, which is unlikely to have happened enough to explain the amount of matter that is required.

### 3.2 Hot, Warm or Cold Dark Matter? (Stan Bovenschen)

We have seen that dark matter should be non-baryonic and weakly interacting. In addition to the types of dark matter explained in section 3.1 we can subdivide dark matter even further in three different models: hot, warm and cold dark matter. The difference in these models has to do with whether or not the dark matter particles were relativistic just before recombination. This difference could have a big influence on the matter structures in later stages of the universe. Therefore, we have to look closely at the CMB, which is a direct remnant of the time of recombination, and to the density distribution of matter throughout the universe.

#### 3.2.1 Hot Dark Matter

Hot dark matter particles are relativistic just before recombination. Around 1980 the hot dark matter model was very popular, since neutrinos seemed to be a good candidate for hot dark matter [25]. People had just discovered that neutrinos were weirdly behaving. Before this time neutrinos were thought of as massless particles. This changed since the discovery of the solar neutrino problem. More specifically, neutrinos are produced in the sun by:



Once we are trying to measure neutrinos on earth we only measure 1/3 of the expected value. The solution to this problem is that neutrinos oscillate, they are constantly changing flavor ( $\nu_e, \nu_\mu, \nu_\tau$ ). This is only possible if neutrinos have mass. And thus people thought neutrinos could be dark matter. However, hot dark matter has as consequence that small scale structures are damped. The density perturbations in the primordial fluid are damped out by the free-streaming, relativistic neutrinos. This has as effect that the initial structures in the early universe are of size  $\lambda_\nu \simeq 40(30\text{eV}/m_\nu) \text{MeV}$ , which is the typical distance a neutrino travels in the lifetime of the universe [26]. Smaller scales, like galaxies, would form later on by fragmentation. We see that this is not the case in our universe and we conclude that  $\lambda_\nu$  for hot dark matter is too large.

Another way of answering the question of whether dark matter in the form of neutrinos is a possibility, is by looking at the density parameter, which indicates what the dominant component of the universe is.  $\Omega_\nu$  is proportional to  $m_\nu$  [27]:

$$\Omega_\nu h^2 = \frac{\sum m_\nu}{93\text{eV}}$$

Since  $m_\nu$  is very small  $\Omega_\nu$  is very small and so if neutrinos where to be dark matter they would be dominated by the other components of  $\Omega$  and they would not play a big role.

Still neutrinos are very helpful in the realm of dark matter since they could possibly be produced by dark matter annihilating in the galaxy. This mostly happens inside objects like planets and stars. Neutrinos are the only particles produced by dark matter that could escape from the initial objects [28]. This way we can use neutrino telescopes to observe dark matter.

#### 3.2.2 Cold Dark Matter

As said before,  $\lambda_\nu$  for hot dark matter is too large. A cold dark matter model has, also, been studied extensively, however here we do not encounter this problem. In the particular model, dark matter was non-relativistic before recombination. This has as an effect that, during the radiation era, matter fluctuations were only growing when their wavelengths are larger than the horizon scale. After that, during the matter dominated era, all fluctuations are growing with the same rate. This way large scale structures can arise [25], as mentioned in section 2.3. There are many cold dark matter candidates, the most prominent of which are Weakly Interacting Massive Particles (WIMPs) and Axions, each with different properties.

For WIMPs it is needless to say that they are weakly interacting (otherwise we could observe them easily) and massive (they need to solve the observed lack of mass). In addition to these obvious properties, they can produce neutrinos, photons, electrons and protons. The latter two can produce more photons through inverse compton scattering. As a result, the CMB could possibly be upscattered by these electrons [28].

Axions are designed to solve the strong CP-problem [29]. Initially the CP-symmetry was supposedly not being violated, until researchers realized that the weak interactions did indeed violate the symmetry. However, we do not know whether the CP-symmetry should or should not be violated for the strong interactions. Experimental research has not been able to give reliable proof of such a violation [30]. There is, however, no reason for it to be conserved, which has led physicists to ask the question as to why it is being conserved. Violation of CP-symmetry causes the axion to have a mass. Both the mass and the strength of the interactions is extremely small, which fits with the predictions of dark matter [31].

Unfortunately the cold dark matter model, also, brings some complications along with it. While on large scales everything appears fine, on smaller scales things are not entirely correct. Galactic velocities on small

structures are too large and there are too many clusters of galaxies. In order to correct for those unwanted properties there are two additional dark matter models: the hot + cold dark matter model and the warm dark matter model, both discussed in section 3.2.3. Of-course, nowadays the  $\Lambda$  cold dark matter ( $\Lambda$ CDM) model, as discussed in section 2.5, is seen as the most plausible model for dark matter.

### 3.2.3 Hot + Cold VS. Warm

We have, previously, seen in this chapter that the hot and the cold dark matter model both have flaws. Hot dark matter arrases the small scales in the early universe. Cold dark matter on the other hand predicts too many clusters of galaxies, in addition to the galactic velocities on small scales being too large. The obvious combination of the two is the hot+cold dark matter model. This model tries to find the right ratio between cold and hot. In 1993 a the following values seemed to agree very well with the observations [32]:

$$\Omega_{cold} = 0.6, \quad \Omega_\nu = 0.3, \quad \Omega_{baryon} = 0.1$$

$$H_0 = 50 \text{ km} \cdot \text{s}^{-1} \cdot \text{Mpc}^{-1}$$

where the hot dark matter candidate is taken to be the neutrino. The density parameter  $\Omega_\nu$ , gives a total neutrino mass of  $m_\nu = 7\text{eV}$ . Despite the agreement with most observations there are a few exceptions. With the given neutrino mass, galaxies may not be able to account for observations of quasars and damped Ly- $\alpha$  systems at high redshift because they form too late [33]. To tune the results a little further, the total neutrino mass in the cold+hot dark matter model has to be lowered from  $7\text{eV}$  to  $\sim 5\text{eV}$ . Because the neutrino oscillation's where not quite well understood in 1995, the total neutrino mass was split up into the tau and muon neutrino masses:

$$m_\tau \approx m_\mu \approx 2.4\text{eV}$$

This way the calculations for large scales seemed to go quite well. On the other hand, in the particle physics point of view, the hot + cold dark matter model was less appreciable, since the calculated masses were too high to be neutrinos.

This problem can be fixed by introducing a hypothetical particle, the sterile neutrino, which could be a form of warm dark matter. Warm dark matter particles have an even lower cross section than neutrinos and they are less abundant. They have a mass of  $\sim 1\text{keV}$ . In this case  $\lambda_\nu$  is much lower [26]. Warm dark matter is not, yet, excluded from being a possible model for dark matter.

## 4 Numerical Simulations in Dark Matter Cosmology (Aliki Litsa)

The numerical simulation techniques used in dark matter research are closely related to the physics of the Early Universe, as described by the cosmological model of inflation and by that of structure formation seeded by matter and density perturbations. As we have, already, mentioned in section 2.2, inflation is the very mechanism that provides the necessary initial conditions in order for the subsequent structure formation to take place, and lead to the creation of all large scale structures observed today. Such conditions include the scale invariant, adiabatic density perturbations, whose growth is first regulated by the radiation itself, and, at later times, by the Dark Matter component of the Universe. The particular perturbations grow during radiation domination, but their growth slows down as they pass the particle horizon. The result is that a characteristic scale is established, which corresponds to the horizon at the moment of transition to the matter dominated era. Since the gravitational potential is the factor which boosts the growth of such matter perturbations, another way of understanding the effect mentioned above, requires an explanation of the way in which the gravitational potential itself evolves. As we can see in Figure 15 the gravitational potential  $\Phi$  remains constant while the modes remain outside the horizon. Modes with a wavenumber  $k \geq k_{eq}$  (where  $k_{eq}$  refers to the characteristic wave-number at matter-radiation equality) cross the horizon during the radiation domination era. The amplitudes of such modes decrease as  $a^{-2}$ , from the time of horizon crossing, until the time of matter-radiation equality, and, therefore, the particular modes enter matter domination significantly decayed. At this point it is important to point out that, while the perturbation growth proceeds logarithmically during radiation domination, it proceeds linearly (and, thus, more intensely) during matter domination. As a result, modes, like the ones mentioned above, which enter matter domination with a significantly decayed gravitational potential do not contribute as much to the formation of large structures in the Universe. On the other hand, modes which satisfy  $k < k_{eq}$ , cross the horizon during the matter era and, therefore, correspond to a gravitational potential which faces minimal decay. The particular modes, enter the matter dominated era with a significant amplitude and are, therefore, able to contribute to structure formation. At the same

time, dark matter fluctuations, below a certain scale, are washed out by random thermal motions. This free-streaming scale corresponds to the comoving distance a particle can travel during the age of the Universe and satisfies  $\lambda \propto m_x^{-1}$  [34].

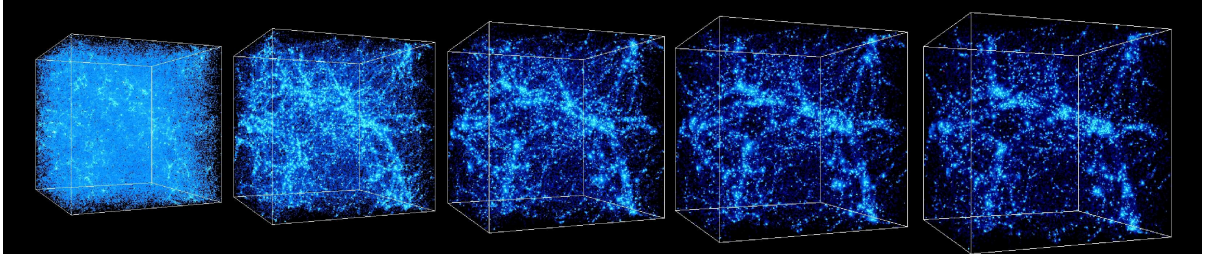


Figure 14: Simulation of formation of the large-scale structure in the universe (Big Bang, inflation, Cold Dark Matter) <http://cosmicweb.uchicago.edu/> Credits: simulations were performed at the National Center for Supercomputer Applications by Andrey Kravtsov (The University of Chicago) and Anatoly Klypin (New Mexico State University).

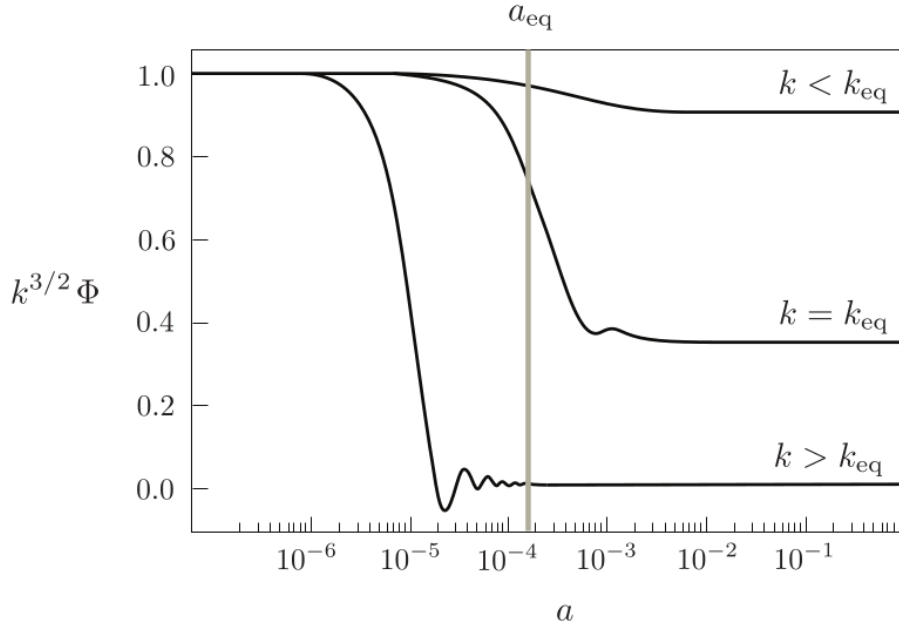


Figure 15: Numerical solutions for the linear evolution of the gravitational potential (taken from Daniel Baumann's notes in Cosmology <https://www.dropbox.com/s/5a6x67n30ssguzv/Chapter4.pdf>)

Having given this short introduction on the processes of perturbation growth and how that affects structure formation, it is time to make the connection with Numerical Simulation techniques and their importance in Dark Matter research. Our conclusions from CMB observations, along with the cosmological theory at hand as described above, indicate that very small structures collapse first and, subsequently, merge to form larger structures. We can, therefore, see that a growth from small to larger and larger objects takes place, ultimately leading to the Universe that is observed today. The baryon acoustic oscillation features, as well as all phenomena related to cosmic scales, emerge from linear or slightly non-linear perturbation growth. As, however, structures get smaller and reach cluster and galactic scales, non-linear growth becomes dominant and the analytical approach of the problem is no longer close to reality. The solution to such a problem is provided by the numerical simulation techniques, which allow the evolution of Dark Matter density fluctuations up to the present day, covering a very large range of length scales (from  $\sim 10$  Gpc to  $\sim 10$  pc). The outcome of numerical simulations is not significantly affected by the composition of dark matter (and by any non-gravitational interactions its ingredients may experience), but rather by the initial velocity distributions of such particles during structure formation. Such distributions do not have a very large effect on large scales,

they can, however, seriously influence smaller scales that may be washed out if the particles are highly relativistic (explained in previous paragraph).

The history of Numerical Simulations in galactic interactions should not necessarily be thought of in terms of computational coding processes, since their first steps took place long before such computational procedures were possible [35]. In 1940, Swedish scientist Erik Holmberg conceived a very creative way of visualizing galaxy interactions, by making use of the fact that both the gravitational and the electric force follow the same inverse square law ( $F \propto \frac{1}{r^2}$ ). Holmberg's experiment included 74 light-bulbs, photocells and galvanometers and some of his results are presented in Figure 16. After measuring the amount of light received by each cell, he manually moved the light-bulbs towards the cell that received the most light, thus simulating galactic motion in the Universe. The years following Holmberg's experiment were characterized by the events of World War II, which boosted progress in all scientific, and especially computational, methods due to the increased military research. However, it wasn't until the early 1970s that numerical simulations in cosmology began to truly prosper, thanks to the newly published cosmological theory of inflation in the scientific community. The initial conditions provided by the particular theory, as explained in the first paragraph of the section, along with subsequent imaging results of galaxies provided by the 3D CfA sky survey (more in section 4.1) gave numerical simulation research the necessary tools for attempting to determine the true composition of the mysterious dark matter component.

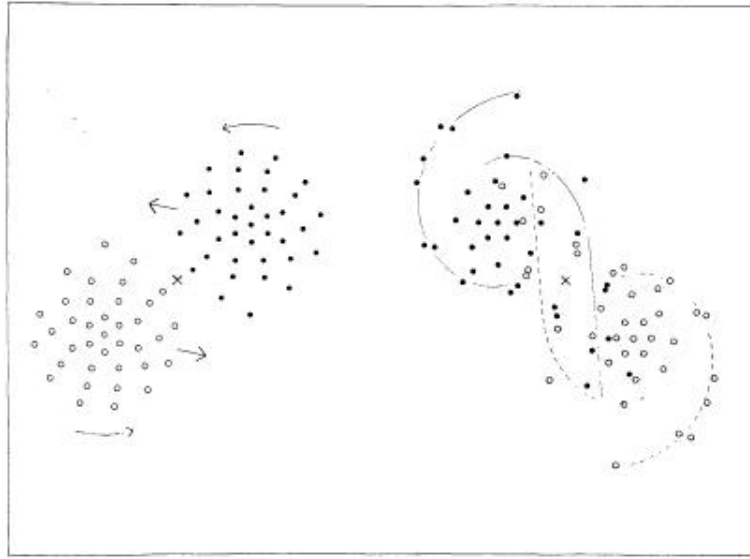


Figure 16: Results of the simulation of a collision between two nebulae. Left panel: two disk-like galaxies approaching. Right panel: after the collision. From Holmberg (1941) [36]

At this point it is important to briefly discuss the particular numerical simulation methods used in order for the result mentioned above to be achieved. In general, cosmological numerical methods include N-body particle simulations, where the gravitational evolution of the particles is determined by the Poisson-Vlasov equations, in a coordinate system which is comoving with the mean expansion of the Universe. The two main techniques include [37]:

- The *Tree Code* technique, where particles are organized in a hierarchical system, depending on their contribution to the gravitational field. More specifically, particles that are very distant from our space-time point of interest, and, therefore, have very low contributions to the gravitational potential of the particular point, are related to low order terms in a multipole expansion of the mass distribution. On the other hand, particles that are closer correspond to higher order terms of the same expansion.
- The *Particle Mesh* method, where particles are placed on a mesh, in order for a density field to be formed. Adapting the particular mesh according to the needs of the problem leads to the formation of high and low density regions.

Such techniques are used for dark matter research in many different scales, from cosmic scale Baryon Acoustic Oscillation simulations to halo simulations in galactic scales. The results of the particular simulations are compared to results from gravitational lensing and CMB observations, in order for conclusions to be drawn.

## 4.1 Excluding Hot Dark Matter with Numerical Simulations (Aliki Litsa)

As we have, already, mentioned in section 3.2.1, Hot Dark Matter does not constitute a viable candidate for the explanation of the Dark Matter properties and effects. Despite their limitations and early stage of evolution, numerical methods in the 1980s played the dominant role for the final dismissal of the HDM model (at least in the case of neutrino dominated models).

In the introductory discussion of this section, we already mentioned the dependence of the free-streaming scale  $\lambda_f$  on the mass of the candidate particle  $m_x$  as  $\lambda_f \propto m_x^{-1}$ . For the case of Hot Dark Matter, the mass of the neutrino candidate  $m_x \sim 30$  eV (according to scientific research carried out in the 1980s) corresponds to a free streaming scale that reaches the size of a large galaxy cluster. Of course, recent measurements of the neutrino mass from neutrino oscillation experiments [38] indicate an even lighter neutrino and, therefore, an even larger  $\lambda_x$ . Since all dark matter fluctuations under the particular scale are damped, the Universe that results from cosmological structure formation, in a HDM model, does not include scales smaller than large galaxy clusters. Therefore, if we assume a HDM cosmological model, the observable Universe today can only be created via top-down procedures, where super-clusters form first, and, then, fragment into galaxies. In the following we are going to examine whether such a Universe can be confirmed by numerical simulation evidence.

The imaging data necessary in order for the numerical simulation efforts to be set in motion were provided in the 1980s, by the 3D CfA redshift survey, which offered information on the positions of a large number of galaxies. During the same decade, various research groups [39], [40], [41], [42] created numerical simulation codes with the purpose of modelling structure growth from the initial conditions of inflation until today. Their goal was to compare their results to data collected by the CfA survey itself, and determine whether the HDM model could be considered a reasonable dark matter model, based on its effects on structure formation on large, as well as small scales. Such numerical simulations of non-linear clustering showed that super-cluster collapse in a HDM Universe must have occurred quite recently at  $z_{sc} < 0.5$ . However, limits on galaxy ages acquired from various globular clusters and other stellar populations indicated that galaxy formation has to have taken place before  $z \sim 3$ . Moreover, since quasars are associated with galaxies, as is suggested by many observations, the abundance of quasars at  $z > 2$  was also inconsistent with the “top-down” neutrino dominated scheme in which superclusters form first:  $z_{sc} > z_{gal}$ .

Figure 17 presents three HDM models, two CDM models, as well as actual observations made by the CfA survey [43]. As we can easily conclude from the plot, HDM simulations provide a rather different Universe density distribution compared to the one we can actually observe. As mentioned in the previous paragraphs, the clustering scale in the case of Hot Dark Matter exceeds the observed scales of galaxy clustering [42], resulting in a much more clustered pattern than the one provided by observations. The reason behind such an effect lies in the fact that, in the case of HDM, the formation of galaxy superclusters, in regions where collapse has taken place, occurs before everything else, due to the very large characteristic scale that is imprinted at horizon crossing (as explained in the introductory part of section 4).

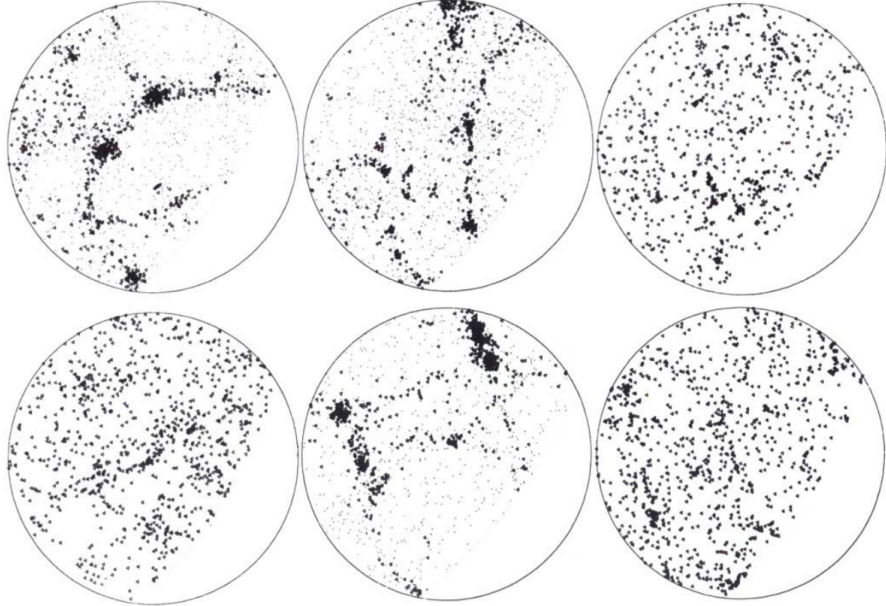


Figure 17: Three HDM models (middle top, middle-bottom and right-bottom panels), two CDM models (left top and left bottom panels) and CfA survey results (right-top) [34]

Further numerical simulations performed during the 1980s [44] made use of the (non-linear) *Pancake model* of Galaxy formation [45], which, also, constitutes a top-down galaxy formation model. The term "pancakes" refers to the thin, dense condensations of gas that are formed from the growth of small inhomogeneities in non-linear gravitational instability theory. After their creation, these condensations, are compressed and heated by shock waves, which leads in their fragmentation into gas clouds. Galaxies and their clusters are formed due to the clumping of these gas clouds. The results of the particular simulations showed that at least 85% of the baryons are so heated by the associated shock that they are unable to condense, and, therefore, unable to attract neutrino halos and form galaxies. This constituted a serious problem for the hot dark matter argument, since, when taking into consideration the primordial nucleosynthesis constraint  $\Omega_b \sim 0.1$ , baryonic matter does not suffice for the production of enough structures which can account for the luminosity observed in the Universe.

Despite any inaccuracies related to the possibly flawed observations of the CfA survey, as well as uncertainties related to galaxy formation, the evidence against the Hot Dark Matter argument were, indeed very convincing from these early stages of dark matter research.

## 4.2 Physics beyond the CDM model (Marnix Heikamp)

### 4.2.1 Problems on small scales

Recently, we have seen that deviations from the CDM model need to be made to fit the found data. These deviations have implications on the structure and evolution of various cosmological systems and are thus topic of debate amongst astronomers. These discussions focus on the impact that baryons have on the dark matter models that exist, and more generally the interplay between the physics that govern the behaviour of both types of matter. We will first look into the observations, or hints towards physics that extends the CDM model, that have recently been made. For a more informative overview of these problems, the reader is suggested to look at [46]. The authors of this review expect the reader to have a basic understanding of galaxies and halos, which could alternatively be obtained by reading section 3.2.1. from [47].

- **Cusp/core problem** If the density of the dark matter halo would be isothermal, it would scale as  $\rho(r) \propto r^{-2}$ . However, it was found that the density profile is governed by the Navarro-Frenk-White (NFW) power-law [48]:

$$\rho(r) = \frac{\rho_s}{(r/r_s)(1+r/r_s)^2}.$$

Here,  $r$  represents the distance to the center and the  $s$  subscript denotes some form of normalization that we shall not investigate. As expected from this,  $\Lambda$ CDM simulations simulations with no other

matter than dark matter, requires the density profiles of the dark matter halo to rise steeply at small radii, such that  $\rho(r) \propto r^{-\gamma}$ , with  $\gamma \simeq 0.8 - 1.4$  in this regime [49]. However, observations show that for most low-mass, dark matter dominated galaxies, the density profile flattens to  $\gamma \simeq 0 - 0.5$  [46]. Additionally, the amount of dark matter that ought to be in the center is higher than what is observed. These observations imply that the halo is more cored than what is expected from the NFW distribution. The consequence of this effect on the rotation curve problem is shown in figure 18. Here, we see that the rotation curve rises quickly for the NFW power-law, whereas observations from two rise slower.

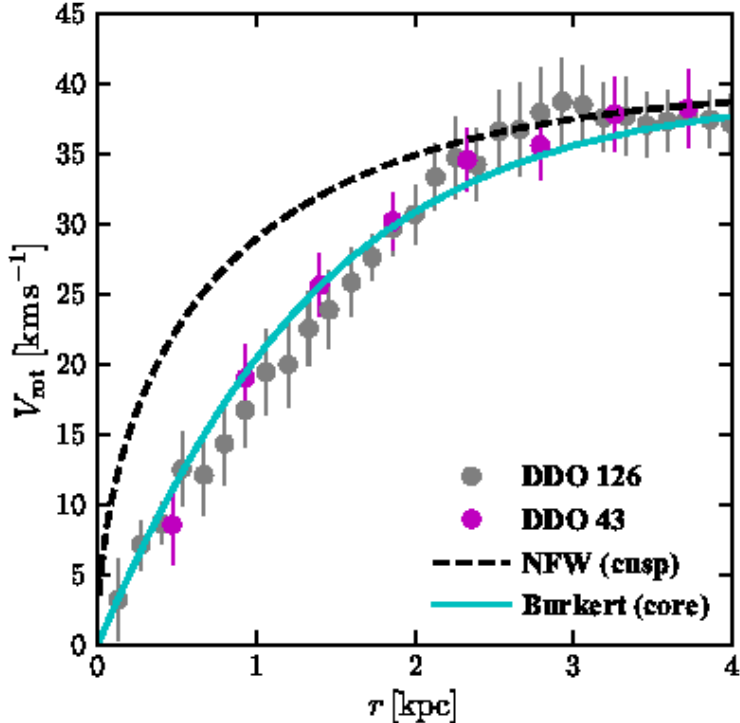


Figure 18: Rotational velocity distribution for various radii according to the NFW model and the fitted data to a flatter density distribution. Figure taken from [46].

- **Missing satellites problem** The former problem arises from the smooth distribution of matter within a halo, whereas the missing satellites problem are coming from the non-smooth distribution parts. Halos form by accretion of smaller halos [47]. However, this accretion process is not complete, causing a substructure that is not smooth [47]. When numerical simulations got good enough resolution to distinguish the different components of a halo, it was found that Milky Way-like galaxies have as many substructures as galaxy clusters have. Even though higher resolution surveys may find more faint dwarf galaxies, the Milky Way does not appear to have enough satellite galaxies to be in accordance with numerical predictions [46].
- **Too big to fail** A direct follow-up of the previous problem is the too big to fail (TBTF) problem. It was found that the discovery that the circular velocities of the largest subhalos in the CDM dark matter-only simulations were too high to be in accordance with the large Milky Way classical dwarfs [47]. This means that these subhalos, which ought to be big enough to make stars and thus be visible, are not found in measurements.
- **Tully-Fisher relation** The Tully-Fisher relation is one of the oldest distance measurements that exists for the Milky Way [50]. It relates the luminosity of a galaxy with the depth of the potential well [47]. However, this relation appears to break down when considering the halo mass and the baryonic mass of a galaxy. It seems that the dwarf galaxies live in smaller halos than expected [47]. Thus, when CDM is the correct way of describing dark matter, there must exist a TBTF problem for small galaxies [47].

#### 4.2.2 Mass of galaxies and dark matter halos

We have just been exposed to four problems that are frequently recurring in literature on problems with CDM. Though it could be the case that these problems are not connected, we aim to find a common interpretation that may explain multiple, or all, stated problems. We find such a solution in the relationship between the masses of the dark matter haloes and the associated galaxies. This relation is especially uncertain on small scales [47].

The last three problems arise as a consequence of the mapping between the observed behaviour, specifically the kinematics, of baryons and the halo mass. We find a discrepancy between the halo that is simulated from CDM and the observed abundance of galaxies. So, in essence, the problem at hand reduces to a counting problem. The former conclusion holds when the current mapping is correct. When this is not the case<sup>1</sup>, the main problem preduces to the cusp/core problem. We know that the ratio for the virial velocity to the velocity of the baryonic tracer is higher in cored halos, so when we know which halos inhabit which galaxies, we would be able to confidently interprete galaxy abundances. I.e., we would know whether we would actually have a counting problem or a cusp/core problem.

It is worth mentioning that when we would be more confident about how to compare galaxies with halos, we would be able to get to the root of the cusp/core problem [47]. The amount of energy that is required to move dark matter towards the edges of a galaxy depends on the characteristics of the potential well, and thus on the halo mass. So, when we would know more about the relation between the galaxies to the halos, we would be able to (dis)prove a CDM + baryon physics interpretation, that can explain the dark matter densities as a function of the galaxy mass. This gives rise to a sense of urgency to find limits on the halo mass.

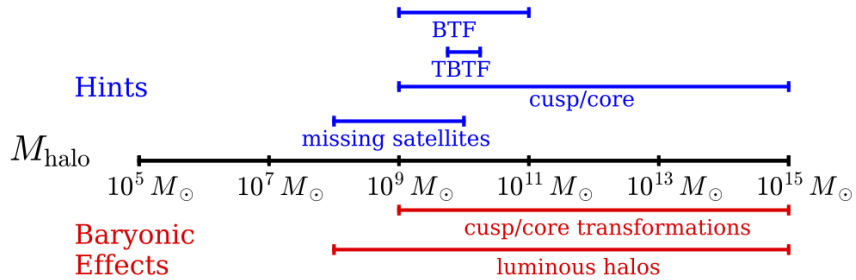


Figure 19: Above: An overview of the various halo masses where hints towards deviations from  $\Lambda$ CDM have been found. Below: An expectation of the range in which baryons are expected to have influence on the structure and evolution of galactic halos [47].

In the top part of figure 19, the different hints towards CDM being an inaccurate description of dark matter at mass scales in the range  $10^{9-15} M_\odot$ .

#### 4.2.3 Considering baryonic matter

The four issues that were put forth in the previous subsection have sparked immense interest from both particle and astrophysicists. Together, the people in these fields have come up with many dark matter models that attempt to adapt dark matter halos with  $M_{vir} \sim 10^{8-15} M_\odot$ . These models mainly consist of predictions that disregard the impact of baryons, for reasons explained in section 3.1. We have readily seen that baryons have a minor contribution to the energy budget of the system, but they do have an import contribution to the dynamics of a system. Thus, we should consider baryons when extending the CDM model to explain the aforementioned problems that arise. We shall thus consider how considering baryons changes all of the mentioned problems.

- **Cusp/core problem** Baryons appeared, from early hydrodynamic simulations, to cool down in halos, and deepened the gravitational well, pulling in dark matter towards the center of a galaxy. More on this method in section 4.3.1 Thus, intensifying the cusp/core problem [47]. Increasing the spatial resolution aided in solving these problems [51]. Unfortunately, simulations have not yet been able to explain the unexpected density profile at low radii. Some simulations create denser cores, whereas others find low density cusps. This signifies that it is yet uncertain how baryonic matter interacts with the dark matter halo and even if baryonic matter is the sole source of this odd finding [47]. Baryons can affect the central

<sup>1</sup>This could for instance occur due to systematic issues or due to a more fundamental error in the CDM simulations, giving rise to the dark matter mass-profile.

density at halo mass scales of order  $10^{9-15} M_{\odot}$  [47, 46]. Thus, studies are continuously performed to uncover the physics that hides in these regimes.

- **Missing satellites problem** The solution towards this problem comes from combining three physical effects. Firstly, we should consider the subhalo mass function. After all, adding baryons to the system allows for a lower dark matter abundance in various ways [47]. Secondly, the mapping of the observed properties to those that arise from simulations. The interested reader is directed to [46] or [47] to find out more about the implications this has. Thirdly, and of most relevance, is the probability that visible baryons may exist in some subhalos. This is of most importance in dwarf galaxies. These reasons combined give convincing arguments towards baryonic matter solving the missing satellite problem. Thus, the new area where research should go into is around and below  $\sim 10^8 M_{\odot}$ . In that regime, galaxy exist without baryons [47].
- **Too big to fail** We already saw that using hydrodynamic simulations of CDM can solve some of the faced issues by introducing baryons. The same type of simulation can fix this problem. Baryons can push dark matter out of the center of the halos, causing the central density to drop. This works on scales around  $10^{10} M_{\odot}$  and does not solve all issues [47]. Especially, Fornax is an interesting case to consider for the interested reader [52].
- **Tully-Fisher relation** The most convincing hint towards solving this issue is by looking into the highest velocity material in galaxies is located in gas with too low column densities to be measured. This causes the velocity measurements to be inaccurate. It is thus appealing to consider the interpretation of the rotation curve as the problem and not the efficiency of star formation [47].

#### 4.2.4 Numerical simulation

We have this far seen that adding baryonic matter aids in some of the presented problems. However, the interaction between baryonic and dark matter is still topic of heated debate. While galaxies form, the present gas cools and falls inwards. This increases the central density and is referred to as 'adiabatic contraction'. This halo contraction appears in most hydrodynamical simulations, but does not succeed in reproducing the observed rotation curves [53, 54]. To fit the numerical result to the observed data, we need a halo that does not contract [53, 55] and potentially even expands [56]. Thus, we need to specify a process that can, at least, counteract this contraction. For instance, the kinematics of the bulk gas can cause considerable fluctuations in the gravitational potential of a galaxy [57, 58]. This leads to a reduced energy density at the inner regions of a galaxy. Indeed, a simulation that attempted to simulate a dwarf galaxy with a cored dark matter profile at  $z = 0$  by applying CDM, having several characteristics of dwarf galaxies [51]. The flattening that was observed in the analysis turned out to be a consequence of small starbursts, located near the center of a young galaxy and creating pockets of fastly expanding gas, which transfer energy from baryonic to dark matter [59].

One of the more noteworthy recent findings on this topic is that including baryon physics brings CDM and non-CDM predictions closer together. We have seen that baryons become relevant for scales  $10^{8-15} M_{\odot}$ , so they affect the halos in figure 19. Thus, although we cannot say that baryons explain all small-scale problems that arise from CDM, we can say that it aids in finding an all-round theory.

### 4.3 Effect of baryons on Numerical Simulations (Stan)

Previously in this chapter we have seen several implications where numerical simulations are needed in our search for dark matter. Dark matter simulations usually are simplified by doing simulations with the dark matter component only. Once we know how this single component universe works, other components are added. Now, to make a simulation of dark matter only is relatively easy because dark matter does not, or barley, interact. Therefore, not taking in account interactions is a pretty good estimate, yet not entirely correct since the dark matter distribution is coupled to the baryonic distribution in the universe. Once adding the baryonic component we need to take into account not only the interactions baryons have with each other but also with dark matter. We know that baryons interact strongly in different ways, due to baryons galaxies can and all other known structures can arise. We need to know exactly how baryons behave throughout the universe in order to be able to make a model with the baryonic component. This model will tell us more about the distributions of dark matter since the two components are gravitationally bound. However, modeling all the baryonic matter of the universe brings some complications with it. Section 4.2.1 gives a detailed description of some of those difficulties. Following in this chapter we will discuss some effects of baryonic matter on dark matter.

#### 4.3.1 Baryonic matter in hydrodynamics

Baryonic matter can be treated like a fluid when the mean free path of a particle is much smaller than the length scale of the fluid:  $\lambda_{mfp} \ll L$ . Also collisions have to happen frequent enough for the fluid to have a distribution close to Maxwellian. This is the case for baryonic gas in most parts of the universe. Since we can neglect viscosity but not the magnetic field of the interstellar medium we have to deal with an ideal magneto-hydrodynamic fluid. This way we can explain several characteristics of baryonic matter in galaxies. The granulation in spiral arms for example arise by the Parker instability, a uniform distribution of the ISM is unstable. Imagine patch of gas with frozen in magnetic field lines where gravity is in the downward direction. Now we insert a perturbation (see figure 20),

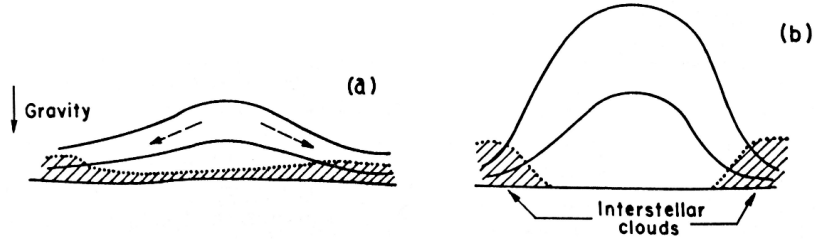


Figure 20: Illustration of the Parker instability. (a) shows a small initial perturbation. (b) shows the result where the interstellar could is separated into two peaces [60].

the magnetic field lines are bend. The gas will 'stream' along the field lines to the side, as a consequence the middle, perturbed, part will have a lower density and become buoyant. The perturbation grows larger and the gas separates to both sides of the perturbation finally the perturbation stops by the tension of the magnetic field lines. A gap within a spiral arm arises [60]. Figure 21 shows a modeled image of galaxy M33 where one can see the granulated spiral arms.

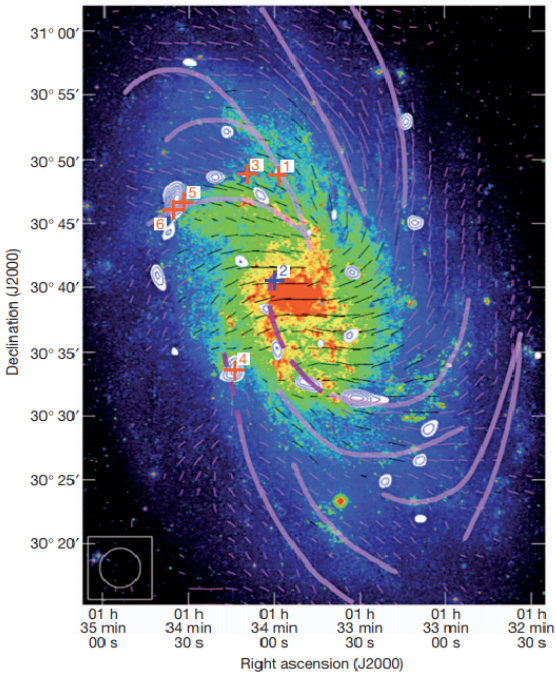


Figure 21: Optical image of galaxy M33. The color decomposition shows different levels of peak intensity of the Gaussian distribution [61]. The fat purple lines are aligned with the spiral arms one can see the irregular shape of baryonic matter as a result of the Parker instability.

Since most of the matter in the universe is in the form of gas in the interstellar medium (ISM) we do not necessarily have to look directly to the mass distribution of more compact objects like stars. Indirectly however, stars and other baryonic objects are influencing the ISM constantly. Supernovae, for example, inject an enormous amount of matter in the ISM. The evolution of the ISM throughout the age of the universe has to do with many parameters, this is hard to model. Therefore techniques are developed to make calculations easier. The Smoothed Particle Hydrodynamics (SPH) approach is an example of such a technique, this will be discussed in the next section.

### 4.3.2 Numerical techniques

One can distinguish two different reference frames for modeling a fluid-dynamic problem. We have the Eulerian approach which has its reference frame at a fixed point in space and the Lagrangian approach which has a reference frame that is co-moving with a fluid element. This difference can also be explained by looking at the derivatives that are used for the fluid dynamical variables in both frames. The relation between the derivatives of both frames is:

$$\frac{dQ}{dt} = \frac{\partial Q}{\partial t} + \mathbf{v} \cdot \nabla Q$$

where  $\frac{dQ}{dt}$  is the Lagrangian derivative and  $\frac{\partial Q}{\partial t}$  the Eulerian derivative.

While doing fluid dynamics we do not necessarily have to use a grid to model astrophysical properties. Instead the SPH technique could be used. This technique uses the Lagrangian, co-moving, approach to calculate the wanted parameters. In addition, it is a particle method which makes use of analytical differentiation of interpolation formulae. In other words, the particles are discretized and obey the implemented interactions between each other, just like a fluid. This results in the fact that the energy and momentum equations become ordinary differential equations [62], these we can understand and interpret. Modeling a hydrodynamics problem by using SPH has certain advantages, namely: this technique is automatically adaptive and has a higher resolution in collapsing regions. The latter is important for the formation of stars, which plays a big role in the history of baryons. SPH also has some disadvantages like the fact that lower density regions are modeled with less precision. Also, there has to be added an artificial viscosity to compensate for the lag of entropy when shocks occur. This extra viscosity makes the method more dissipative [37]. In order to get rid of those disadvantages people are looking for improvements of the SPH technique.

Another well known technique for modeling baryonic matter is Adaptive Mesh Refinement (AMR). This technique is based on the Eulerian frame, where the fluid flow is discretized in space. Here the grid where the Euler equations are calculated on is adapted to be finer on the places where a higher accuracy is needed. This method has as advantages that it describes shocks very well and it has little noise. Also instabilities, like the Parker instability, are well modeled. However the AMR algorithm is more complex and it therefore takes longer to run [37].

Now it is clear that both of those methods have some flaws. The obvious solution for the problems of both techniques is combining the two. This results in an adaptive moving grid [63]. With this combined technique we are finally able to start thinking about modeling galaxies.

### 4.3.3 Modeling galaxies

In several early simulations of the galaxy distribution, all the galaxies were approximated to behave the same way. This is of course not true since there are so many micro- and macroscopic effects that we have to account for. It is possible to precisely model galaxies by using the previously described techniques and our knowledge of magneto-hydrodynamics. When 'creating' a galaxy one has to take into account that a galaxy is not adiabatic, galaxies are for example cooling due to radiation emission. For this non-adiabatic processes cooling functions can be implemented to calculate what will happen to, for example, the cooling rate as function of density and the temperature [64].

Due to the non-adiabaticity of the galaxy, certain regions will cool. The gas pressure will decrease and star formation can happen by fragmentation. The adaptable grid will make sure that we will capture every effect that plays a role on these smaller scales. For star formation to happen a gas could will need to meet the Jeans limit, where a cloud of a certain density is smaller than its Jeans length. Once this is the case we can estimate the formation time by the free fall timescale. By implementing a Schmidt law we can estimate how often star formation will happen [65]. Star formation is, however, not one hundred percent efficient. It turns out that the star formation rate (SFR) per free fall time is only:  $SFR/\tau_{ff} \approx 0.01$  [66]. In galaxies we also have to deal with dying stars, which can be really messy. Especially supernovae and jets from neutron stars are ejecting huge amounts of material in the interstellar medium. These processes are called Feedback

processes. Feedback happens on small scales, yet it can have a great effect on larger, galactic scale [67]. Figure 22 is an example of a modeled galaxy where all the previously discussed properties are processed.

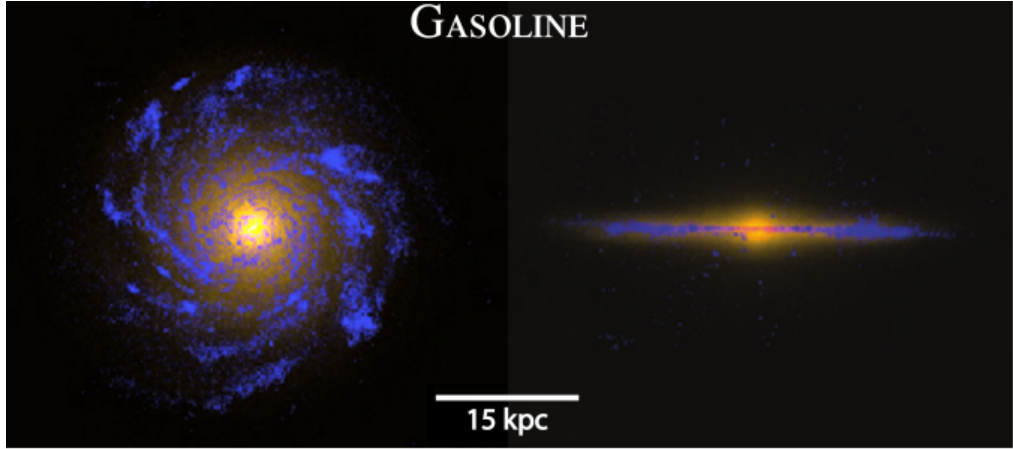


Figure 22: Optical and UV composite images of the Eris galaxy, a Milky Way like galaxy. [67]

#### 4.3.4 Stellar streams

A stellar stream is a band of many stars that are aligned within the galaxy. Every star in the stream follows the same track around the galaxy. These stars are supposedly all drifting away from the same cluster where they formed. The stellar streams have more or less a constant stellar density along its length. The existence of star streams was determined in 1996 [68]. Later, in 2001, it became clear that the streams form from tidal deformation in clusters [69].

Both the cold and warm dark matter models (as explained in section 3.2.2 and 3.2.3) predict that smaller structures than dwarf galaxies (i.e.  $M < 10^7 M_\odot$ ) will be completely dark matter dominated, these dark matter halos are obviously hard to locate since they do not emit light. A possible way of detecting them could be by looking at the stellar streams. Once coming close enough, the small scale dark matter halos would be able to gravitationally interact with the stars in the stream by pushing them out of the stream. This way a gap appears in the stream which we will be able to detect [70].

However, we have to be careful with our conclusions since a gap in such a stellar stream could also be an effect of baryonic matter. In figure 23 the stellar stream Pal 5 that has been modeled and displayed. The figure shows a clear gap at  $-0^\circ.4 < \phi < 0^\circ.2$  which is exactly what we are looking for to detect dark matter sub halos. Unfortunately this gap has been made by the Milky Way bar and not by a dark matter halo [71]. It is therefore of great importance to distinguish baryonic effects from dark matter effects.

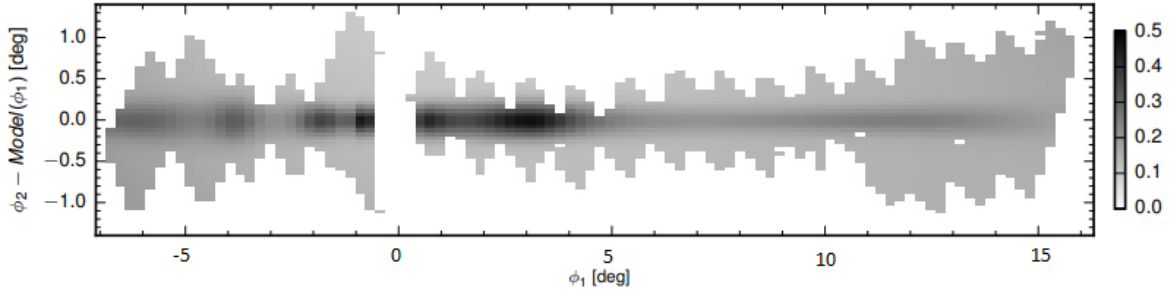


Figure 23: Density distribution of stars in the Pal 5 stellar stream, predicted by the maximum likelihood model. With a gap at  $-0^\circ.4 < \phi < 0^\circ.2$  which is swept away by the Milky Way bar [71].

### 4.3.5 Future considerations (Marnix Heikamp)

Slowly, though steadily, more and more studies are investigating this contribution of baryons to the theory of dark matter. Two astronomical systems are frequently used: isolated dwarf galaxies and Milky Way like galaxies. The former is chosen as the computational costs for a high spatial resolution result is relatively low compared to more massive systems. Considering that hydrodynamic simulations are, when important processes such as radiative transfer are ignored, at least an order of magnitude more complicated to execute than dark matter-only simulations [47]. This makes the choice for isolated dwarf galaxies apparent. Studying Milky Way like galaxies is relevant due to the missing satellites and TBTF problems [47]. Additionally, studying stellar streams will provide more insights in the nature of dark matter.

## 5 particle physics solutions

## 6 Modified Newtonian Dynamics (MOND) (Marnix Heikamp)

So far, we have explained the characteristics of dark matter. However, we have not yet considered the possibility of an alternative theory for gravity. After all, the problem that arises from flat rotation curves can be solved by applying at least one of two different solution concepts: 1. There exists invisible matter 2. Newton's laws do not hold for galaxies [72]. Concept 1 points to dark matter, concept 2 to a different theory of gravity. An example of such a theory is the modified Newtonian dynamics (MOND). It turns out that such a theory can explain the unexpected shape of the rotation curve. In this section, we will describe the theory, and consecutively elaborate on the complications that MOND faces; arising from gravitational waves and the bullet cluster.

### 6.1 Milgrom's law

Although Newton's laws have been widely tested in high-acceleration environments, they haven't been tested in the realm where objects undergo low acceleration, which happens at the outer edges of galaxies [73]. Thus, we can introduce a constant  $a_0$ , with units of acceleration, and state that Newtonian physics applies when  $a_0 \gg a$ . Then, this paves the way towards a modified expression for the Newtonian force:

$$F_N = m\mu\left(\frac{a}{a_0}\right)a, \quad (1)$$

where  $m$  is the gravitational mass of the object,  $a$  is the acceleration, and the interpolation function is:

$$\mu(x) \rightarrow \begin{cases} 1 & \text{for } x \gg 1 \\ x & \text{for } x \ll 1 \end{cases} \quad (2)$$

So, in the regime where Newtonian physics breaks down according to MOND,  $a \ll a_0$ , we find that:

$$F_N = m\frac{a^2}{a_0}.$$

Now, for objects with mass  $m$  in a circular orbit (which we approximate the stars in our galaxy to follow), we have that:

$$\begin{aligned} \frac{GMm}{r^2} &= m\frac{(v^2/r)^2}{a_0} \\ v^4 &= \frac{GMma_0r^2}{mr^2} \\ &= GMa_0 \end{aligned}$$

Here,  $a_0$  is experimentally found to be  $\sim 10^{-8} \text{ ms}^{-2}$  [72, 73]. This indeed gives rise to a rotation velocity that is independent of  $r$ , such that the rotation velocity is flat, implying there is no need for dark matter.

## 6.2 Conservation of momentum

We can, thus, see that Milgrom's law, as written in equation 1, solves the problems that arise from the  $\Lambda$ CDM interpretation and which will be discussed in the following sections. However, this is merely a law, which should be derived from a universal force law and, furthermore, does not uphold the principle of conservation of momentum. Let us consider a system in which two masses,  $m_1$  and  $m_2$  are small enough to be in the weak acceleration limit, and in rest on the x-axis. Now, we can express the change in momentum of the system as follows:

$$\begin{aligned}\dot{p} &= \dot{p}_1 + \dot{p}_2 = m_1 \dot{v}_1 - m_2 \dot{v}_2 = ma_1 - ma_2 \\ &= m_1 \sqrt{\frac{F_N a_0}{m_1}} - m_2 \sqrt{\frac{F_N a_0}{m_2}} = \sqrt{F_N a_0} (\sqrt{m_1} - \sqrt{m_2}).\end{aligned}$$

We can immediately see that this does not equal 0 when  $m_1 \neq m_2$ , thus violating the principle of the conservation of momentum. Thus, equation 1 cannot be more than an approximation of a more heuristic force law. Such a law would have to be derived from a variational and action principle, leading to a modified Newtonian dynamics (MOND) theory<sup>2</sup>.

To change the dynamics such that they will give Milgrom's law, the classical action provides a good starting point. We describe a system in which a set of particles move in a gravitational field that arises from the matter density,  $\rho = \sum_i m_i \delta(x - x_i)$  and is linked to a potential,  $\Phi_N$ , such that:

$$S_N = S_{\text{kin}} + S_{\text{in}} + S_{\text{grav}} = \int \frac{\rho v}{2} d^3 x dt - \int \rho \Phi d^3 x dt - \int \frac{|\nabla \Phi_N|^2}{8\pi G} d^3 x dt$$

Now, we know that  $d^2 x / dt^2 = -\nabla \Phi_N$ , which can be used to find  $\nabla^2 \Phi_N = 4\pi G \rho$ . We can now modify the gravitational action. When we do this, the equation of motion remains in tact, but we will find a different Poisson equation [72]. For the gravitational action, we derive:

$$S_{\text{grav, BM}} = - \int \frac{a_0^2 F(|\nabla \Phi|^2 a_0^2)}{8\pi G} d^3 x dt,$$

where  $F$  represents any dimensionless function. We can vary this with respect to  $\Phi$ , to find:

$$\nabla \left[ \mu \left( \frac{|\nabla \Phi|}{a_0} \right) \nabla \Phi \right] = 4\pi G \rho,$$

where  $\mu(x) = F(\sqrt{x})$  and  $\mu(x)$  still satisfies equation 2. Thus, when  $|\nabla \Phi| \ll a_0$ , we find that the potential becomes non-linear, which is contradictory to general relativity, which predicts linear equations in the weak-field limit [74]. This means that we can constrain MOND by considering general relativity and gravitational waves (GWs) in particular.

## 6.3 Gravitational waves

There are two ways in which MOND can alter gravitational wave physics[74]. Firstly, MOND can violate the equivalence principle as it is an acceleration based theory. This would imply that GWs can propagate with a speed that is less than the speed of light. Secondly, as we just saw that the equations are non-linear in the weak-field limit, GWs could then be explained by non-linear equations.

Let's first delve into the first claim. When GWs propagate with  $c_g < 1$ , where the speed of light,  $c = 1$ , we must conclude that the arrival times of an electromagnetic signal and the gravitational wave that originate from the same source cannot be the same. However, a recent detection of a GW coming from an inspiraling neutron star binary, of which an electromagnetic counterpart was measured, was made and the time between the arrivals turned out to be 1.7 seconds [75, 76]. This implies that the speed of gravitational waves is equal to the speed of light as that time difference can be explained by the Shapiro time [77]. Additionally, when  $c_g < 1$ , highly energetic cosmic rays that travel with  $v \rightarrow 1$  will lose energy via Cherenkov radiation with a rate dependent on  $1 - c_g$ . Observing such cosmic rays on Earth allows for a lower bound on  $c_g$  causing the rate dependence to be  $1 - c_g \lesssim 10^{-15}$  [78, 79]. Thus, it is very unlikely that the speed of gravitational waves is less than the speed of light. In some MOND theories, the speed of gravitational waves depends on the gravitational potential and cannot generically be set to 1, thus making these theories inaccurate.

<sup>2</sup>We shall discuss the classical level, and refrain from discussing the weak-field limit, which is more properly described by modified Einstein Dynamics.

Regarding the second claim on the non-linearity of the gravitational wave dynamics, we can deduce the following. When these dynamics would indeed be non-linear, the GWs that originate from black hole mergers could interact with themselves. However, LIGO's observation of a black hole merger in 2014 showed no such interaction as the observed signal was consistent with predictions made by general relativity [80]. Therefore, we don't require such a scrambling effect, so we would expect that gravitational waves should satisfy linear equations of motion in the weak-field limit.

We can thus conclude that MOND theories must be heavily constrained by the principles arising from gravitational waves. This implies that it becomes questionable whether MOND is an applicable theory, let alone explain the problems that the theory of dark matter attempts to explain.

## 6.4 Bullet cluster

The bullet cluster (1E0657-56) merger is a cluster that has given many insights, which we have hinted towards before. Here, we will consider the implications that it has on MOND. At the simplest of levels, this system seems to disprove MOND [81]. In MOND, gravity is expected to traverse the trace of light and would thus not be able to explain the lensing characteristics of the bullet cluster [82]. This happens because the gravitational center is not aligned with the photometric center, indicating that spacetime might be anisotropic [83]. However, bullet clusters also turn out to be difficult for  $\Lambda$ CDM, as the collision velocity ( $\sim 4700 \text{ kms}^{-1}$ ) is extremely unlikely in this theory [84]. A way around this problem for MOND has been proposed by [85] and has been verified by [83]. Here, a metric is conceived that is comparable to the Schwarzschild metric, with one change. The spatial distance  $r$  is replaced by a distance,  $R = r(f(v(r)))$ . Under certain assumptions, this simplifies to MOND as proposed by Milgrom. This form of MOND can explain the characteristics of the bullet cluster and fits the rotation curve data as well. This may thus explain the missing matter problem [86].

We thus need a special form of MOND to explain the problems that are more generally explained by the theory of dark matter. When also considering the consequences of the recent GWs detection, it becomes tricky to use the theory of MOND as these detections give strong constraints on the possible MOND theories.

## References

- [1] F. Zwicky. Die Rotverschiebung von extragalaktischen Nebeln. *Helv. Phys. Acta*, 6:110–127, 1933. [Gen. Rel. Grav. 41, 207(2009)].
- [2] Vera C. Rubin and W. Kent Ford, Jr. Rotation of the Andromeda Nebula from a Spectroscopic Survey of Emission Regions. *Astrophys. J.*, 159:379–403, 1970.
- [3] Jian Qi Shen. The dark-baryonic matter mass relation for observational... *Gen. Rel. Grav.*, 50(6):73, 2018.
- [4] Mads T. Frandsen and Jonas Petersen. Investigating Dark Matter and MOND Models with Galactic Rotation Curve Data. 2018.
- [5] KG Begeman, AH Broeils, and RH Sanders. Extended rotation curves of spiral galaxies: Dark haloes and modified dynamics. *Monthly Notices of the Royal Astronomical Society*, 249(3):523–537, 1991.
- [6] Stacy McGaugh, Federico Lelli, and Jim Schombert. Radial Acceleration Relation in Rotationally Supported Galaxies. *Phys. Rev. Lett.*, 117(20):201101, 2016.
- [7] Nathália Cibirka et al. RELICS: Strong Lensing analysis of the galaxy clusters Abell S295, Abell 697, MACS J0025.4-1222, and MACS J0159.8-0849. 2018.
- [8] J. Ehlers and P. Schneider. Gravitational lensing. In *Proceedings, 13th International Conference on General Relativity and Gravitation: Cordoba, Argentina, June 28-July 4, 1992*, pages 21–40, 1993.
- [9] Douglas Clowe, Maruša Bradač, Anthony H Gonzalez, Maxim Markevitch, Scott W Randall, Christine Jones, and Dennis Zaritsky. A direct empirical proof of the existence of dark matter. *The Astrophysical Journal Letters*, 648(2):L109, 2006.
- [10] Maxim Markevitch, AH Gonzalez, D Clowe, A Vikhlinin, W Forman, C Jones, S Murray, and W Tucker. Direct constraints on the dark matter self-interaction cross section from the merging galaxy cluster 1e 0657-56. *The Astrophysical Journal*, 606(2):819, 2004.

- [11] Maxim Markevitch and Alexey Vikhlinin. Shocks and cold fronts in galaxy clusters. *Physics Reports*, 443(1):1–53, 2007.
- [12] J. R. Brownstein and J. W. Moffat. The Bullet Cluster 1E0657-558 evidence shows Modified Gravity in the absence of Dark Matter. *Mon. Not. Roy. Astron. Soc.*, 382:29–47, 2007.
- [13] Daniel J. Eisenstein et al. Detection of the Baryon Acoustic Peak in the Large-Scale Correlation Function of SDSS Luminous Red Galaxies. *Astrophys. J.*, 633:560–574, 2005.
- [14] P. A. R. Ade et al. Planck 2015 results. XIII. Cosmological parameters. *Astron. Astrophys.*, 594:A13, 2016.
- [15] P. J. E. Peebles and J. T. Yu. Primeval adiabatic perturbation in an expanding universe. *Astrophys. J.*, 162:815–836, 1970.
- [16] J. R. Bond and G. Efstathiou. Cosmic background radiation anisotropies in universes dominated by nonbaryonic dark matter. *Astrophys. J.*, 285:L45–L48, 1984.
- [17] Wayne Hu and Naoshi Sugiyama. Small scale cosmological perturbations: An Analytic approach. *Astrophys. J.*, 471:542–570, 1996.
- [18] Daniel J. Eisenstein and Wayne Hu. Baryonic features in the matter transfer function. *Astrophys. J.*, 496:605, 1998.
- [19] R. F. vom Marttens, L. Casarini, W. S. Hipólito-Ricaldi, and W. Zimdahl. CMB and matter power spectra with non-linear dark-sector interactions. *JCAP*, 1701(01):050, 2017.
- [20] Adam G. Riess, Lucas M. Macri, Samantha L. Hoffmann, Dan Scolnic, Stefano Casertano, Alexei V. Filippenko, Brad E. Tucker, Mark J. Reid, David O. Jones, Jeffrey M. Silverman, Ryan Chornock, Peter Challis, Wenlong Yuan, Peter J. Brown, and Ryan J. Foley. A 2.4 *The Astrophysical Journal*, 826(1):56, 2016.
- [21] Planck Collaboration. Planck 2015 results - xiii. cosmological parameters. *A&A*, 594:A13, 2016.
- [22] Wilmar Cardona, Martin Kunz, and Valeria Pettorino. Determining  $H_0$  with Bayesian hyper-parameters. *JCAP*, 1703(03):056, 2017.
- [23] Antonio Enea Romano. Hubble trouble or Hubble bubble? 2016.
- [24] Io Oddershov, Steen Hannestad, and Jacob Brandbyge. The variance of the locally measured Hubble parameter explained with different estimators. *JCAP*, 1703(03):022, 2017.
- [25] M. Davis, G. Efstathiou, C. S. Frenk, and S. D. M. White. The evolution of large-scale structure in a universe dominated by cold dark matter. *apj*, 292:371–394, May 1985.
- [26] Scott Dodelson and Lawrence M. Widrow. Sterile neutrinos as dark matter. *Phys. Rev. Lett.*, 72:17–20, Jan 1994.
- [27] O. Lahav and A.R. Liddle. The Cosmological Parameters. 21, 2013.
- [28] N. Fornengo. Dark matter overview. In *25th European Cosmic Ray Symposium (ECRS 2016) Turin, Italy, September 04-09, 2016*, 2016.
- [29] R. D. Peccei and Helen R. Quinn. CP conservation in the presence of pseudoparticles. *Phys. Rev. Lett.*, 38:1440–1443, Jun 1977.
- [30] John Preskill, Mark B. Wise, and Frank Wilczek. Cosmology of the invisible axion. *Physics Letters B*, 120(1):127 – 132, 1983.
- [31] Michael Dine and Willy Fischler. The not-so-harmless axion. *Physics Letters B*, 120(1):137 – 141, 1983.
- [32] A. Klypin, J. Holtzman, J. Primack, and E. Regos. Structure Formation with Cold plus Hot Dark Matter. *apj*, 416:1, October 1993.
- [33] Joel R. Primack, Jon Holtzman, Anatoly Klypin, and David O. Caldwell. Cold + hot dark matter cosmology with  $m(\nu_\mu) \approx m(\nu_\tau) \approx 2.4$  ev. *Phys. Rev. Lett.*, 74:2160–2163, Mar 1995.

- [34] Carlos S Frenk and Simon DM White. Dark matter and cosmic structure. *Annalen der Physik*, 524(9–10):507–534, 2012.
- [35] Gianfranco Bertone and Dan Hooper. A history of dark matter. *arXiv preprint arXiv:1605.04909*, 2016.
- [36] Erik Holmberg. On the clustering tendencies among the nebulae. ii. a study of encounters between laboratory models of stellar systems by a new integration procedure. *The Astrophysical Journal*, 94:385, 1941.
- [37] Michael Kuhlen, Mark Vogelsberger, and Raul Angulo. Numerical Simulations of the Dark Universe: State of the Art and the Next Decade. *Phys. Dark Univ.*, 1:50–93, 2012.
- [38] Antonio Marrone, Francesco Capozzi, Eleonora Di Valentino, Eligio Lisi, Alessandro Melchiorri, and Antonio Palazzo. Global constraints on neutrino masses and their ordering. *AIP Conf. Proc.*, 1894(1):020015, 2017.
- [39] Carlos S. Frenk, Simon D. M. White, and Marc Davis. Nonlinear evolution of large-scale structure in the universe. *Astrophys. J.*, 271:417, 1983.
- [40] Ya. B. Zeldovich, J. Einasto, and S. F. Shandarin. Giant Voids in the Universe. *Nature*, 300:407–413, 1982.
- [41] A Dekel and SJ Aarseth. The spatial correlation function of galaxies confronted with theoretical scenarios. *The Astrophysical Journal*, 283:1–23, 1984.
- [42] Simon DM White, CS Frenk, and Marc Davis. Clustering in a neutrino-dominated universe. *The Astrophysical Journal*, 274:L1–L5, 1983.
- [43] John Huchra, Marc Davis, David Latham, and J Tonry. A survey of galaxy redshifts. iv-the data. *The Astrophysical Journal Supplement Series*, 52:89–119, 1983.
- [44] PR Shapiro, C Struck-Marcell, and AL Melott. Pancakes and the formation of galaxies in a neutrino-dominated universe. *The Astrophysical Journal*, 275:413–429, 1983.
- [45] YA B Zel'Dovich. Gravitational instability: An approximate theory for large density perturbations. *Astronomy and astrophysics*, 5:84–89, 1970.
- [46] James S. Bullock and Michael Boylan-Kolchin. Small-Scale Challenges to the  $\Lambda$ CDM Paradigm. *Ann. Rev. Astron. Astrophys.*, 55:343–387, 2017.
- [47] Matthew R. Buckley and Annika H. G. Peter. Gravitational probes of dark matter physics. 2017.
- [48] Julio F Navarro, Carlos S Frenk, and Simon DM White. A universal density profile from hierarchical clustering. *The Astrophysical Journal*, 490(2):493, 1997.
- [49] Julio F. Navarro, Aaron Ludlow, Volker Springel, Jie Wang, Mark Vogelsberger, Simon D. M. White, Adrian Jenkins, Carlos S. Frenk, and Amina Helmi. The Diversity and Similarity of Cold Dark Matter Halos. *Mon. Not. Roy. Astron. Soc.*, 402:21, 2010.
- [50] R Brent Tully and J Richard Fisher. A new method of determining distances to galaxies. *Astronomy and Astrophysics*, 54:661–673, 1977.
- [51] Fabio Governato et al. At the heart of the matter: the origin of bulgeless dwarf galaxies and Dark Matter cores. *Nature*, 463:203–206, 2010.
- [52] Mei-Yu Wang, Louis E. Strigari, Mark R. Lovell, Carlos S. Frenk, and Andrew R. Zentner. Mass assembly history and infall time of the Fornax dwarf spheroidal galaxy. *Mon. Not. Roy. Astron. Soc.*, 457(4):4248–4261, 2016.
- [53] Oleg Y. Gnedin, Daniel Ceverino, Nickolay Y. Gnedin, Anatoly A. Klypin, Andrey V. Kravtsov, Robyn Levine, Daisuke Nagai, and Gustavo Yepes. Halo Contraction Effect in Hydrodynamic Simulations of Galaxy Formation. 2011.
- [54] Andrea V. Maccio', Greg Stinson, Chris B. Brook, James Wadsley, H. M. P. Couchman, Sijing Shen, Brad K. Gibson, and Tom Quinn. Halo expansion in cosmological hydro simulations: towards a baryonic solution of the cusp/core problem in massive spirals. *Astrophys. J.*, 744:L9, 2012.

- [55] S. Courteau, A. A. a Dutton, F. van den Bosch, L. A. MacArthur, A. Dekel, D. H. McIntosh, and Daniel A. Dale. Scaling Relations of Spiral Galaxies. *Astrophys. J.*, 671:203, 2007.
- [56] Aaron A. Dutton, Charlie Conroy, Frank C. van den Bosch, Luc Simard, Trevor Mendel, Stephane Courteau, Avishai Dekel, Surhud More, and Francisco Prada. Dark halo response and the stellar initial mass function in early-type and late-type galaxies. *Mon. Not. Roy. Astron. Soc.*, 416:322, 2011.
- [57] Sergey Mashchenko, H. M. P. Couchman, and James Wadsley. Cosmological puzzle resolved by stellar feedback in high redshift galaxies. *Nature*, 442:539, 2006.
- [58] Sergey Mashchenko, James Wadsley, and H. M. P. Couchman. Stellar Feedback in Dwarf Galaxy Formation. *Science*, 319:174, 2008.
- [59] Andrew Pontzen and Fabio Governato. How supernova feedback turns dark matter cusps into cores. *Mon. Not. Roy. Astron. Soc.*, 421:3464, 2012.
- [60] Arnab Rai Choudhuri. *The Physics of Fluids and Plasmas: An Introduction for Astrophysicists*. Cambridge University Press, 1998.
- [61] Hua bai Li and Thomas Henning. The alignment of molecular cloud magnetic fields with the spiral arms in m33. *Nature*, 479:499–501, 2011.
- [62] J. J. Monaghan. Smoothed particle hydrodynamics. *Annual Review of Astronomy and Astrophysics*, 30(1):543–574, 1992.
- [63] N. Y. Gnedin. Softened Lagrangian hydrodynamics for cosmology. *apjs*, 97:231–257, April 1995.
- [64] G. J. Ferland, K. T. Korista, D. A. Verner, J. W. Ferguson, J. B. Kingdon, and E. M. Verner. Cloudy 90: Numerical simulation of plasmas and their spectra. *Publications of the Astronomical Society of the Pacific*, 110(749):761, 1998.
- [65] M. Schmidt. The Rate of Star Formation. *apj*, 129:243, March 1959.
- [66] Mark R. Krumholz and Jonathan C. Tan. Slow star formation in dense gas: Evidence and implications. *The Astrophysical Journal*, 654(1):304, 2007.
- [67] J. Guedes, S. Callegari, P. Madau, and L. Mayer. Forming Realistic Late-type Spirals in a  $\Lambda$ CDM Universe: The Eris Simulation. *apj*, 742:76, December 2011.
- [68] R. Klement, B. Fuchs, and H.-W. Rix. Identifying stellar streams in the first rave public data release. *The Astrophysical Journal*, 685(1):261, 2008.
- [69] Michael Odenkirchen, Eva K. Grebel, Constance M. Rockosi, Walter Dehnen, Rodrigo Ibata, Hans-Walter Rix, Andrea Stolte, Christian Wolf, Jr. John E. Anderson, Neta A. Bahcall, Jon Brinkmann, István Csabai, G. Hennessy, Robert B. Hindsley, Željko Ivezić, Robert H. Lupton, Jeffrey A. Munn, Jeffrey R. Pier, Chris Stoughton, and Donald G. York. Detection of massive tidal tails around the globular cluster palomar 5 with Sloan Digital Sky Survey commissioning data. *The Astrophysical Journal Letters*, 548(2):L165, 2001.
- [70] Nilanjan Banik, Gianfranco Bertone, Jo Bovy, and Nassim Bozorgnia. Probing the nature of dark matter particles with stellar streams. 04 2018.
- [71] Denis Erkal, Sergey E. Koposov, and Vasily Belokurov. A sharper view of pal 5’s tails: discovery of stream perturbations with a novel non-parametric technique. *Monthly Notices of the Royal Astronomical Society*, 470(1):60–84, 2017.
- [72] Benoit Famaey and Stacy McGaugh. Modified Newtonian Dynamics (MOND): Observational Phenomenology and Relativistic Extensions. *Living Rev. Rel.*, 15:10, 2012.
- [73] Mordehai Milgrom. MOND-theoretical aspects. *New Astron. Rev.*, 46:741–753, 2002.
- [74] Paul M. Chesler and Abraham Loeb. Constraining Relativistic Generalizations of Modified Newtonian Dynamics with Gravitational Waves. *Phys. Rev. Lett.*, 119(3):031102, 2017.
- [75] B.P. Abbott et al. GW170817: Observation of Gravitational Waves from a Binary Neutron Star Inspiral. *Phys. Rev. Lett.*, 119(16):161101, 2017.

- [76] S. Boran, S. Desai, E. O. Kahya, and R. P. Woodard. GW170817 Falsifies Dark Matter Emulators. *Phys. Rev.*, D97(4):041501, 2018.
- [77] Irwin I. Shapiro. Fourth Test of General Relativity. *Phys. Rev. Lett.*, 13:789–791, 1964.
- [78] Guy D. Moore and Ann E. Nelson. Lower bound on the propagation speed of gravity from gravitational Cherenkov radiation. *JHEP*, 09:023, 2001.
- [79] Joshua W. Elliott, Guy D. Moore, and Horace Stoica. Constraining the new Aether: Gravitational Cerenkov radiation. *JHEP*, 08:066, 2005.
- [80] B. P. Abbott et al. Observation of Gravitational Waves from a Binary Black Hole Merger. *Phys. Rev. Lett.*, 116(6):061102, 2016.
- [81] Craig Lage and Glennys R Farrar. The bullet cluster is not a cosmological anomaly. *Journal of Cosmology and Astroparticle Physics*, 2015(02):038, 2015.
- [82] Garry W Angus, Huan Yuan Shan, Hong Sheng Zhao, and Benoit Famaey. On the proof of dark matter, the law of gravity, and the mass of neutrinos. *The Astrophysical Journal Letters*, 654(1):L13, 2006.
- [83] Zhe Chang, Ming-Hua Li, Xin Li, Hai-Nan Lin, and Sai Wang. Finslerian MOND versus the Strong Gravitational Lensing of the Early-type Galaxies. *Eur. Phys. J.*, C73:2550, 2013.
- [84] Stacy S. McGaugh. A Novel Test of the Modified Newtonian Dynamics with Gas Rich Galaxies. *Phys. Rev. Lett.*, 106:121303, 2011. [Erratum: *Phys. Rev. Lett.* 107, 229901 (2011)].
- [85] Xin Li, Ming-Hua Li, Hai-Nan Lin, and Zhe Chang. Finslerian MOND vs. observations of Bullet Cluster 1E0657-558. *Mon. Not. Roy. Astron. Soc.*, 428(4):2939–2948, 2013.
- [86] Zhe Chang, Ming-Hua Li, Xin Li, Hai-Nan Lin, and Sai Wang. Effects of spacetime anisotropy on the galaxy rotation curves. *Eur. Phys. J.*, C73:2447, 2013.